PHYSICAL REVIEW D **80,** 064006 (2009)

Extreme- and intermediate-mass ratio inspirals in dynamical Chern-Simons modified gravity

Carlos F. Sopuerta[1] and Nicolás Yunes[2]

[1]*Institut de Ciències de l'Espai (CSIC-IEEC), Facultat de Ciències, Campus UAB, Torre C5 parells, Bellaterra, 08193 Barcelona, Spain*

[2]*Physics Department, Princeton University, Princeton, New Jersey 08544, USA*

(Received 28 April 2009; published 2 September 2009)

Chern-Simons modified gravity is a four-dimensional, effective theory that descends both from string theory and loop quantum gravity, and that corrects the Einstein-Hilbert action by adding the product of a scalar field and the parity-violating, Pontryagin density. The Chern-Simons modification deforms the gravitational field of spinning black holes, which is now described by a modified Kerr geometry whose multipole moments deviate from the Kerr ones only at the fourth multipole $\ell = 4$. This paper investigates possible signatures of this theory in the gravitational-wave emission produced in the inspiral of stellar compact objects into massive black holes, both for intermediate- and extreme-mass ratios. We use the *semirelativistic* approximation, where the trajectory of the small compact object is modeled via geodesics of the massive black hole geometry, while the gravitational waveforms are obtained from a multipolar decomposition of the radiative field. The main Chern-Simons corrections to the waveforms arise from modifications to the geodesic trajectories, which in turn are due to changes to the massive black hole geometry, and manifest themselves as an accumulating dephasing relative to the general relativistic case. We also explore the propagation and the stress-energy tensor of gravitational waves in this theory, using the short-wavelength approximation. We find that, although this tensor has the same form as in general relativity, the energy and angular momentum balance laws are indeed modified through the stress-energy tensor of the Chern-Simons scalar field. These balance laws could be used to describe the inspiral through adiabatic changes in the orbital parameters, which in turn would enhance the dephasing effect. Gravitational-wave observations of intermediate- or extreme-mass-ratio inspirals with advanced ground detectors or with the Laser Interferometer Space Antenna could use such dephasing to test the dynamical theory to unprecedented levels, thus beginning the era of gravitational-wave tests of effective quantum gravity theories.

DOI: 10.1103/PhysRevD.80.064006 PACS numbers: 04.30.−w, 04.25.−g, 04.25.Nx, 04.50.Kd

I. INTRODUCTION

The experimental verification of symmetry breaking is one of the most powerful tools to understand in which direction to extend the current canon toward more fundamental physical theories. For example, the experimental confirmation of the violation of charge conjugation, parity transformation and time-reversal symmetries in elementary particle interactions forced the improvement of the quantum field theory of particles into what is today the standard model. Similarly, violation of symmetries in gravitational interactions can push toward generalizations of general relativity (GR) by providing the first experimental evidence of high-energy extensions.

Gravitational parity violation can be tuned by the inclusion of a Pontryagin term in the Einstein-Hilbert action, which defines an effective, four-dimensional gravitational theory: Chern-Simons (CS) modified gravity [1]. In fact, the inclusion of such a term in the action is inescapable in four-dimensional compactifications of perturbative string theory (i.e. type I, IIb, heterotic, etc.) due to the Green-Schwarz anomaly-canceling mechanism [2]. This fact can also be extended to the nonperturbative sector in the presence of Ramond-Ramond scalars (D-instanton charges) due to duality symmetries [3]. Such a term also arises naturally in loop quantum gravity when the Barbero-Immirzi parameter is promoted to a scalar field coupled to the Nieh-Yan invariant [4–6]. More generically, the Pontryagin correction to the action also arises unavoidably in effective field theories, as it has been recently shown in the context of cosmological inflation [7].

The action of dynamical CS modified gravity (DCSMG) consists of the Einstein-Hilbert term plus the product of a scalar field and the Pontryagin density (the contraction of the Riemann curvature tensor with its dual), plus the action for this scalar field and/or other matter fields. The CS corrections modify the field equations for the metric components by adding two extra terms to the Einstein equations: the so-called *C tensor* and a stress-energy tensor for the scalar field. The C tensor depends on derivatives of the CS scalar and the contraction of the Levi-Civita tensor with covariant derivatives of the Ricci tensor and the dual Riemann tensor. In addition, the variation of the action with respect to the CS scalar field leads to an equation of

motion for this field, which is sourced by the Pontryagin density.

The CS gravitational modification has been investigated mostly in the nondynamical framework, in which the scalar field is nondynamical (there is no kinetic term for it in the action), and hence it is assumed to be an *a priori* prescribed spacetime function. Such studies include an analysis of well-posedness [8], exact solutions [1,9], approximate solutions [1,10–14], matter interactions [15,16], cosmology [3,17–19], and astrophysical tests [20–22]. Nondynamical CS modified gravity has been shown to be theoretically problematic in relation to Schwarzschild black hole perturbation theory [23], the existence of stationary and axisymmetric solutions [24], and the uniqueness of solutions of the theory [25].

The detailed study of the dynamical formulation of CS modified gravity has only recently begun. This paper is the second in a series that deals with the details of the dynamics of CS modified, spinning black holes. In the first paper [25], henceforth paper I, an approximate solution was found for a spinning black hole, using the slow-rotation approximation and a small-coupling approximation. The first type of approximation restricts attention to black holes with small angular momentum per unit mass, while the second one allows one to search for small CS deformations of known GR solutions. The new solution corresponds to a deformation of the Kerr metric whose deviations fall off with a high power of the distance to the black hole.

In this paper, we concentrate on the study of intermediate- and extreme-mass-ratio inspirals (IMRIs and EMRIs, respectively) in the context of DCSMG. Such systems consist of a small compact object (SCO) (with masses in the range 1–$30M_{\odot}$) orbiting around a (spinning) massive black hole (MBH) (with masses in the range 10^4–$10^7M_{\odot}$) in the case of EMRIs, and an intermediate-mass black hole (IMBH) (with masses in the range 10^2–$10^4M_{\odot}$; see [26] for a review on the evidence of the existence of IMBHs) in the case of IMRIs. Another IMRI possibility would be that of an IMBH falling into a MBH, a system with obviously also an intermediate-mass ratio (see [27] and references therein). The mass ratios involved are then in the range $(10^{-2}$–$10^{-4})$ for IMRIs and $(10^{-4}$–$10^{-7})$ for EMRIs.

EMRIs (and IMRIs involving an IMBH-MBH binary) are important sources of gravitational waves (GWs) for future space detectors [28] as the Laser Interferometer Space Antenna (LISA) [29–33], whereas IMRIs are important sources for second generation ground based detectors (see [34,35]), such as Advanced LIGO [36] and Advanced VIRGO [37], and for future planned third generation detectors as the Einstein Telescope [38]. Both IMRIs and EMRIs are high-precision sources that can produce a high number of detectable GW cycles. Hence, GW observations of these systems will have a strong impact on astrophysics, cosmology, and fundamental physics [39–41], the latter of which we shall be concerned with here (see [42] for a detailed account of IMRI and EMRI astrophysics and related science).

The construction of IMRI/EMRI waveforms for data analysis purposes is a difficult problem since the accuracy needed for detection and extraction of physical parameters is quite high. For the case of EMRIs, techniques for constructing sufficiently accurate templates for *detection* is currently underway, mainly through the use of the adiabatic approximation [43–52]. Methods to build sufficiently accurate templates for *parameter estimation* have not yet been fully developed, the main difficulty being that one requires a more precise treatment of the self-gravity of the SCO and its impact on the gravitational waveform. For IMRIs, one might have to incorporate the finite-size effects of the SCO on the waveforms, since the mass ratio is not so extreme.

In this article, we will use a simpler method to describe EMRIs, the so-called *semirelativistic* approximation [53], in which the motion of the SCO is taken to be geodesic on the MBH spacetime (Kerr in GR and modified Kerr in DCSMG) and the GWs are computed using a multipolar decomposition [54] assuming that they propagate from the source to the observer in flat space. In the radiation zone, the different multipoles are fully determined by the trajectory of the SCO and its derivatives. Such a scheme therefore neglects radiation-reaction effects that scale with the square of the mass ratio of the system. One can add these effects by using different types of approximations that provide expressions for the change of the *constants* of motion in terms of the properties of the GWs emitted [55–58]. Given the nature of the semirelativistic approximation, it is clear that it has accuracy limitations in the sense that it is not good enough for creating a template bank for parameter estimation. However, as we argue in this paper, it will suffice to understand the type of corrections induced in CS modified EMRIs and IMRIs.

We begin by considering the trajectory of the SCO in the MBH background. We find that the motion of a test particle in DCSMG is *exactly* described by the geodesic equations, as in GR. Trajectory modifications are thus produced entirely by the modified geometry of the MBH background, which is here described by the modified Kerr solution found in paper I. These modifications include corrections to the geodesic equations and to the fundamental frequencies of motion. Since the CS correction to the MBH background is a high-order, strong-field effect, the multipoles of the hole are not corrected up to the $\ell = 4$ multipole, suggesting that a test of the Kerr geometry might be difficult with LISA. This theory is thus an interesting illustration of how the geometry of a MBH can be changed by physically well-motivated curvature corrections to the Einstein-Hilbert action.

We continue with a discussion of GW generation in DCSMG, which for EMRIs and IMRIs can be studied using black hole perturbation theory. We see that the

perturbations, and hence the GW emission, are indeed corrected by the C tensor and the stress-energy tensor of the CS scalar field. Expanding in the mass ratio and in the CS coupling constants that act as CS deformation parameters, we find that the second-order corrections to GW emission are the usual GR radiation-reaction effect (proportional to the square of the mass ratio) and a new CS correction (proportional to the product of the mass ratio and the CS coupling constants). Depending on the strength of these constants, this modification could be much smaller than, comparable to, or bigger than radiation-reaction effects. In this paper, as a first exploratory study of these questions, we shall neglect these second-order effects, and thus, we shall model GW emission through the usual GR multipolar expansion. Modifications to GW emission, hence, originate from corrections to the geodesic trajectories of the SCO, which in turn arise due to the modified MBH geometry.

With these tools at hand, we then proceed to solve the geodesic equations for a set of EMRI systems and compare the GWs generated in GR with those generated in DCSMG. Figure 1 shows the changes in the waveforms, essentially an accumulating dephasing, for the last 11 minutes of the plus-polarized waveform after 128 days of evolution for the system described in the caption. The GR waveforms are here denoted with a dotted blue line, while the DCSMG waveforms are denoted with a solid black line. The amount of CS dephasing depends on the specific type of orbit and the magnitude of the CS correction, where we generically find a strong effect on the waveform for orbits that spend the longest close to the MBH.

Our study suggests that a GW observation of highly relativistic IMRIs and EMRIs could place constraints on

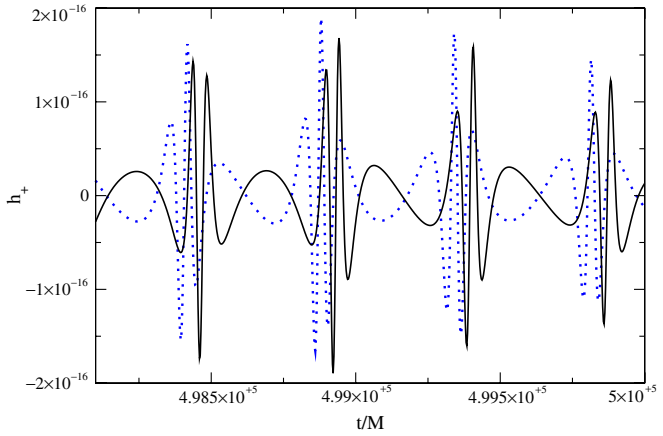

FIG. 1 (color online). Plus-polarized waveform as a function of time using a Kerr background (dotted blue line) and the CS deformed metric (solid black line). The pericenter is at $r = 6M$ (with $M = 4.5 \times 10^6 M_\odot$), the inclination angle is 0.3 radians, the spin angular momentum is $J/M^2 = 0.4$, while the CS coupling strength is set at $\xi/M^4 = 0.4$. For more details on this system see Sec. V A and for further details on the precise definition of the CS coupling strength see Sec. II.

the dynamical theory that are orders of magnitude larger than current binary pulsar ones [25]. This constraint depends strongly on how relativistic the system is, as well as on the signal-to-noise ratio of the event, and on the total mass of the system. Including radiation-reaction effects should allow us to search, for the first time, for radiative effects associated with the CS scalar field in the neighborhood of compact objects, which is simply not possible with binary pulsars (see [59,60] for detailed information on tests of gravitational theories, in particular, for tests with pulsars). To confirm these expectations a detailed analysis using appropriate data analysis tools is required, but shall not be performed here.

Remarkably, a physically well-motivated curvature-squared correction to GR, like the one studied here, seems to lead to spinning black hole solutions and GWs that resemble the GR prediction quite closely. This fact suggests that GW detectors should be able to detect GWs, irrespective of whether GR or CS waveform templates are employed. As long as the precise nature of the massive compact object or the structure of the true gravitational theory does not modify the GR predictions enough, as we show is the case in DCSMG, the current data analysis algorithms should be able to extract the signals by using purely GR templates and performing incoherent searches of the data in short segments (e.g. roughly three weeks). However, in our case, the CS modification may prevent us from *connecting* these segments together and associate them to a specific EMRI or IMRI system.

Although the study of GWs emitted by EMRIs associated to non-Kerr backgrounds is not new [61,62], the analysis presented here is the first one to consider an alternative to the Kerr metric that derives from a concrete and physically well-motivated alternative theory of gravity (based on high-order curvature corrections to GR). In contrast to arbitrary quasi-Kerr deformations, the black hole solution considered here deviates from Kerr significantly *only in the strong-field* region and only through gravitomagnetic components. Thus, mismatches between GW signals of EMRIs in this background (and in DCSMG) and GWs in Kerr (and in GR) are dominated exclusively by truly strong-field effects and not by subleading, weak-field corrections. Tests of such modified theories seem to require not only the detection of a sufficiently large number of segments, but also the reconstruction of a unique GW signal.

We conclude this paper with a discussion of the role of radiation-reaction effects in DCSMG through the short-wavelength approximation. In particular, we investigate how one could introduce these effects in the adiabatic approximation (that is, in the regime where the rate of change of the orbital parameters due to GW emission is much smaller than the typical orbital periods) in order to construct truly inspiraling IMRI/EMRI waveforms in DCSMG. This calculations typically involve the computa-

tion of fluxes of energy and angular momentum in order to estimate the change in the *constants* of motion. One possible way of estimating these fluxes is through the effective stress-energy tensor of the gravitational waves, which is defined in the so-called short-wavelength approximation (see [63] and references therein). We find that the effective GW stress-energy tensor, the Isaacson tensor, and thus the GW stress-energy loss, is the *same* in DCSMG as in GR. The backreaction of this loss on the background, however, is different in DCSMG because GW losses must here be supplemented by the stress-energy distribution of the CS scalar field. Truly inspiraling IMRI/EMRI waveforms can then be constructed in DCSMG by supplementing the semirelativistic approximation with adiabatic changes of the orbital parameters due to *both* GW and CS scalar field stress-energy losses.

The details of this study are organized as follows: Section II discusses the basics of DCSMG, its linearized version, the study of GW polarization in this theory, and reviews the small-coupling approximation; Sec. III describes test-particle motion in DCSMG, including the expression of the modified Kerr solution, and the derivation of the equations for timelike geodesics. We also discuss how the fundamental frequencies of geodesic motion are modified due to the changes in the MBH metric; Sec. IV describes GW generation in the modified theory and the type of semirelativistic approximation that we use; in Sec. V we apply the previous results to construct numerically the trajectories and waveforms; Sec. VI discusses GW propagation in the short-wavelength approximation and shows that the GW energy momentum tensor and emission in DCSMG is the same as in GR. We also calculate the stress-energy emission due to the CS scalar field and the modification to the background (averaged) scalar field due to terms quadratic in the perturbation of the Riemann tensor; Sec. VII concludes and discusses future research directions.

We use the following conventions throughout this work. Greek letters and a semicolon are used to denote indices and covariant differentiation, respectively, on the four-dimensional spacetime. We denote covariant differentiation with respect to the background metric by $\bar{\nabla}_\mu B_\nu$ or by $B_{\nu|\mu}$. Partial differentiation with respect to the coordinate x^μ is denoted as $\partial_\mu B_\nu$ or $B_{\nu,\mu}$. Symmetrization and antisymmetrization are denoted with parentheses and square brackets around the indices, respectively, such as $A_{(\mu\nu)} := [A_{\mu\nu} + A_{\nu\mu}]/2$ and $A_{[\mu\nu]} := [A_{\mu\nu} - A_{\nu\mu}]/2$. We use the metric signature $(-,+,+,+)$ and geometric units in which $G = c = 1$.

II. CHERN-SIMONS MODIFIED GRAVITY

In this section we describe the formulation of CS modified gravity that we shall employ and establish some basic notation (see also paper I). We begin with a discussion of the basics of the modified theory, but refer the reader to paper I or the upcoming review [64] for further details. We continue with a review of the linearized theory in DCSMG. Then we study basic properties of GW polarization in DCSMG, illustrated with plane waves. Finally we introduce the small-coupling approximation.

A. General formulation

The starting point is the action of DCSMG:

$$S = S_{\rm EH} + S_{\rm CS} + S_{(\vartheta)} + S_{\rm mat}, \tag{1}$$

where

$$\begin{aligned} S_{\rm EH} &= \kappa \int d^4x\sqrt{-{\rm g}}R, \\ S_{\rm CS} &= \frac{\alpha}{4}\int d^4x\sqrt{-{\rm g}}\quad \vartheta\, {}^*RR, \\ S_{(\vartheta)} &= -\frac{\beta}{2}\int d^4x\sqrt{-{\rm g}}[{\rm g}^{\mu\nu}(\nabla_\mu\vartheta)(\nabla_\nu\vartheta) + 2V(\vartheta)], \\ S_{\rm mat} &= \int d^4x\sqrt{-{\rm g}}\mathcal{L}_{\rm mat}, \end{aligned} \tag{2}$$

where $\kappa = (16\pi G)^{-1}$ is the gravitational constant; α is the coupling constant of the CS scalar field ϑ with the parity-violating Pontryagin density ${}^*RR$ given by

$${}^*RR := R_{\alpha\beta\gamma\delta}{}^*R^{\alpha\beta\gamma\delta} = \tfrac{1}{2}\epsilon^{\alpha\beta\mu\nu}R_{\alpha\beta\gamma\delta}R^{\gamma\delta}{}_{\mu\nu}, \tag{3}$$

where the asterisk denotes the dual tensor, constructed using the antisymmetric Levi-Civita tensor $\epsilon^{\alpha\beta\mu\nu}$; β is a constant that determines the gravitational strength of the CS scalar field stress-energy distribution. The different terms in Eq. (1) correspond to the following: the first one is the Einstein-Hilbert action; the second one is the CS gravitational correction; the third one is the CS scalar field action, which contains a kinetic and a potential term $V(\vartheta)$, both of which distinguish the dynamical formulation from previous ones; and the fourth one is the action corresponding to matter degrees of freedom.

Upon variation of the action with respect to the metric and the CS scalar, we obtain the field equations of DCSMG:

$$G_{\mu\nu} + \frac{\alpha}{\kappa}C_{\mu\nu} = \frac{1}{2\kappa}(T^{\rm mat}_{\mu\nu} + T^{(\vartheta)}_{\mu\nu}), \tag{4}$$

$$\beta\Box\vartheta = \beta\frac{dV}{d\vartheta} - \frac{\alpha}{4}{}^*RR, \tag{5}$$

where $T^{\rm mat}_{\mu\nu}$ is the matter stress-energy tensor and $T^{(\vartheta)}_{\mu\nu}$ is the stress-energy of the CS scalar field, given by

$$T^{(\vartheta)}_{\mu\nu} = \beta[(\nabla_\mu\vartheta)(\nabla_\nu\vartheta) - \tfrac{1}{2}\mathrm{g}_{\mu\nu}(\nabla^\sigma\vartheta)(\nabla_\sigma\vartheta) - \mathrm{g}_{\mu\nu}V(\vartheta)]. \tag{6}$$

In this work we will study only the case in which the potential term associated with the CS scalar field is assumed to vanish[1] ($V = 0$). The tensor $C^{\mu\nu}$ (the so-called *C tensor*) in Eq. (4) can be split into two parts, $C^{\mu\nu} = C_1^{\mu\nu} + C_2^{\mu\nu}$, where

$$\begin{aligned} C_1^{\alpha\beta} &= (\nabla_\sigma\vartheta)\epsilon^{\sigma\delta\nu(\alpha}\nabla_\nu R^{\beta)}{}_\delta, \\ C_2^{\alpha\beta} &= (\nabla_\sigma\nabla_\delta\vartheta)^* R^{\delta(\alpha\beta)\sigma}. \end{aligned} \tag{7}$$

As we have mentioned, there are two conceptually distinct CS modified gravity theories: a dynamical version and a nondynamical version. In the former, the quantities α and β are arbitrary, and the field equations are the ones we have given in Eqs. (4) and (5). The nondynamical version is characterized by the choice $\beta = 0$ at the level of the action, and thus the evolution equation for the CS scalar becomes a differential constraint on the space of allowed solutions, the so-called Pontryagin constraint ${}^*RR = 0$.

The nondynamical theory presents a certain number of difficulties that make it less physically interesting than the dynamical formulation [23–25]. In the former, one can show that single-parity perturbation modes lead to an overconstrained system of perturbed equations, disallowing generic quasinormal ringing [23]. Moreover, spinning black hole solutions were found to be strongly restricted by the Pontryagin constraint, in some cases also leading to an overconstrained system [24]. Finally, the freedom in the choice of the CS scalar field was shown to lead to nonunique solutions with infinite energy scalars in paper I [25].

Most of the difficulties and arbitrariness of the nondynamical theory can be avoided by adopting the dynamical framework, i.e. DCSMG theory, where the freedom regarding the CS scalar field reduces to the choice of initial conditions. The stationary state of the CS scalar has been seen to be independent of the initial conditions, being determined only by the metric through the source term in the evolution equation for ϑ [25]. For these reasons, we choose here to study the dynamical formulation.

B. Radiation zone expansion

GWs are properly defined only at future null infinity, but in practice one can define such waves perturbatively in the so-called radiation zone, i.e. several GW wavelengths away from the location of the sources. In order to study GWs in DCSMG, let us split the spacetime metric as the sum of a background metric $\bar{\mathrm{g}}_{\mu\nu}$ (we use the overbar to denote objects associated with the background) and a metric (GW) perturbation $h_{\mu\nu}$:

$$\mathrm{g}_{\mu\nu} = \bar{\mathrm{g}}_{\mu\nu} + \epsilon h_{\mu\nu} + \mathcal{O}(\epsilon^2), \tag{8}$$

where ϵ is a bookkeeping perturbative parameter, associated to the smallness of the metric perturbation relative to the background, which we use to label the order of the approximation.

In this section and in other parts of this paper, we simplify equations by using the Lorenz gauge

$$(h^{\mu\nu} - \tfrac{1}{2}h\bar{\mathrm{g}}^{\mu\nu})_{|\nu} = 0, \tag{9}$$

where $h = \bar{\mathrm{g}}^{\mu\nu}h_{\mu\nu}$ is the trace of the metric perturbation with respect to the background. Since we shall be at first interested in computing the DCSMG corrections to gravitational radiation measured by observers in the radiation zone, we shall restrict the gauge further by supplementing it with the trace-free condition

$$h = 0, \tag{10}$$

leading to a transverse-traceless gauge far away from the source.

The restriction to the radiation zone in this section allows us to focus on a flat background $\bar{\mathrm{g}}_{\mu\nu} = \eta_{\mu\nu}$, a good approximation sufficiently far away from the source. In Secs. III and IV we will lift this restriction and consider more generic backgrounds. When considering generic backgrounds we will also find it essential to decompose ϑ into a background field $\bar{\vartheta}$ and a perturbation. For the present case of a flat background, this is not necessary, since the background field must necessarily reduce to a constant. We expect then ϑ to be sourced by the metric perturbation, leading to certain leading-order corrections to the equations of motion for wave generation.

In this gauge and with a flat background, the leading-order Riemann, dual Riemann, and Ricci tensors are [66]

$$R_{\mu\nu\rho\sigma} = \epsilon[h_{\sigma[\mu,\nu]\rho} - h_{\rho[\mu,\nu]\sigma}] + \mathcal{O}(\epsilon^2), \tag{11}$$

$${}^*R^{\delta\alpha\beta\gamma} = \epsilon\bar{\epsilon}^{\delta\mu\nu\alpha}h_\nu{}^{[\beta,\gamma]}{}_\mu + \mathcal{O}(\epsilon^2), \tag{12}$$

$$R_{\mu\nu} = -\frac{\epsilon}{2}\Box_\eta h_{\mu\nu} + \mathcal{O}(\epsilon^2), \tag{13}$$

respectively, where $\Box_\eta = \eta^{\mu\nu}\partial_\mu\partial_\nu$ is the flat-space d'Alembertian and $\bar{\epsilon}^{\mu\nu\alpha\beta}$ is the flat-space Levi-Civita symbol or tensor density (not to be confused with the bookkeeping parameter ϵ). The leading-order C tensor in this gauge is then

[1] In string theory, the ϑ field corresponds to the axion, which possess a shift symmetry and a vanishing potential along certain *flat* directions. The axion is a moduli field, which, when stabilized by supersymmetry breaking [65], acquires a nonflat potential. Such a potential would arise at the scale of supersymmetry breaking, which is much larger than the gravitational scale.

$$C_{\mu\nu} = -\frac{\epsilon}{2}(\partial_\sigma\vartheta)\bar{\epsilon}^{\sigma\delta\xi}{}_{(\mu}\Box_\eta h_{\nu)\delta,\xi} - \frac{\epsilon}{2}(\partial^\gamma_\sigma\vartheta)\bar{\epsilon}^{\sigma\delta\xi}{}_{(\mu|}[h_{\xi\gamma,|\nu)\delta} - h_{\nu)\xi,\gamma\delta}] + \mathcal{O}(\epsilon^2). \tag{14}$$

Combining these leading-order expressions, we find that the modified field equations in trace-reversed form become

$$-\frac{1}{\kappa}\bar{T}_{\mu\nu} = \epsilon\Box_\eta h_{\mu\nu} + \frac{\alpha}{\kappa}(\partial_\sigma\vartheta)\epsilon\bar{\epsilon}^{\sigma\delta\xi}{}_{(\mu}\Box_\eta h_{\nu)\delta,\xi} + \frac{\alpha}{\kappa}(\partial^\gamma_\sigma\vartheta)\epsilon\bar{\epsilon}^{\sigma\delta\xi}{}_{(\mu}[h_{\xi\gamma,|\nu)\delta} - h_{\nu)\xi,\gamma\delta}], + \mathcal{O}(\epsilon^2), \tag{15}$$

$$\beta\Box\vartheta = -\frac{\alpha}{2}\epsilon^2\bar{\epsilon}^{\alpha\beta\mu\nu}h_{\alpha\delta,\gamma\beta}h_\nu{}^{[\gamma,\delta]}{}_\mu + \mathcal{O}(\epsilon^3), \tag{16}$$

where $\bar{T}_{\mu\nu} = T_{\mu\nu} - (1/2)\eta_{\mu\nu}T$ is the trace-reversed version of the total stress-energy tensor $T_{\mu\nu} = T^{\rm mat}_{\mu\nu} + T^{(\vartheta)}_{\mu\nu}$. We see clearly that the metric perturbation is sourced by $\bar{T}_{\mu\nu}$, which implies that the contribution of this source must also be of leading-order $\mathcal{O}(\epsilon)$, while the scalar field is sourced by the Pontryagin density that is of leading $\mathcal{O}(\epsilon^2)$ in the radiation zone. Note in this regard that, as we already pointed out, we have not yet introduced a perturbative expansion for the CS scalar field.

C. Gravitational-wave polarizations

Since we are dealing with a different theory of gravity, one must be specially careful of not assuming GW properties that hold only in GR. In this sense, a question of particular relevance that arises with alternative theories of gravity refers to the number of independent GW polarizations. DCSMG possesses an extra degree of freedom described by the CS scalar field, and thus, additional GW polarizations could in principle be present. This issue can be investigated by following the pioneering work of [67,68], where a formalism is presented to study far-field gravitational radiation in any metric theories of gravity. One then finds that only six possible independent GW polarizations are possible, leading to a suitable classification [the so-called $E(2)$ classification] of alternative theories.

In this framework one focuses on the propagation of monochromatic plane waves in the radiation zone (i.e. assuming weak fields) and their effect on test masses. This can be done by considering the geodesic deviation equation (see e.g. [63,69]), which describes the relative acceleration between nearby geodesics:

$$U^\rho\nabla_\rho(U^\sigma\nabla_\sigma X^\mu) := A^\mu = R^\mu{}_{\nu\rho\sigma}U^\nu U^\rho X^\sigma, \tag{17}$$

where U^μ is the test mass four-velocity and X^μ is the so-called deviation vector, which describes the displacement between test masses. Different GW polarizations will induce a different deviation effect on test masses, that can be classified via the structure of the Riemann tensor. Thus, the $E(2)$ classification sorts metric theories based on the vanishing or nonvanishing of the Newman-Penrose scalars (in an appropriate Newman-Penrose null basis), associated with the Riemann curvature tensor, which can be shown to describe GW polarizations.

Applying this procedure to DCSMG (one can use the formulas of the linear theory presented above), we find that only the two GW polarizations also present in GR are observable far away from sources. Such a study had not yet been performed in DCSMG, although several investigations exist in the nondynamical theory: [1] proved the above result in the nondynamical theory for a linearly time-dependent scalar field, while [12,13] extended this result to generic time-dependent scalars. This fact can be further illustrated by studying the properties of exact plane waves (solution of the full field equations). We have included such a study in Appendix A.

D. The small-coupling approximation

This approximation consists of expanding the modified field equations in the dimensionless parameter $\zeta = \mathcal{O}(\xi/M^4)$, where $\xi := \alpha^2/(\beta\kappa)$ and M is a characteristic mass associated with the particular system under consideration. To that end, we assume that ζ is a *small* perturbation parameter associated with the CS gravitational modifications and the physical system under study. As we did in the linearized theory, ζ will be also used as a bookkeeping parameter for labeling the different perturbative orders, but we will set it to unity at the end of our calculations. Combining this approximation with the linear one we can set up a two-parameter perturbative scheme, in ζ and ϵ, that in the context of the DCSMG was introduced in paper I and we refer to this work for details (for a general discussion about multiparameter perturbation theory see [70], and in the context of GR see [71–75]). As in paper I, the order counting shall assume that $\beta = \mathcal{O}(\alpha)$ such that $\alpha/\beta = \mathcal{O}(1)$ and $\xi = \mathcal{O}(\alpha/\kappa)$ without loss of generality.

The metric perturbations $h_{\mu\nu}$ and the CS scalar field θ can then be expanded as

$$h_{\mu\nu} = \sum_{a,b}\epsilon^a\zeta^b h^{(a,b)}_{\mu\nu}, \qquad \vartheta = \sum_{a,b}\epsilon^a\zeta^b\vartheta^{(a,b)}, \tag{18}$$

where $h^{(a,b)}_{\mu\nu}$ and $\vartheta^{(a,b)}$ stand for the perturbations of $\mathcal{O}(\xi^a, \zeta^b)$ and $a + b \geq 1$. Introducing these expansions in the field equations one can then set up a bootstrapping method that consists of first solving the evolution equation for the CS scalar field and then using this solution in the modified Einstein field equations to solve for the CS correction to the metric perturbations. In order to prevent the existence of metric perturbations whose dominant behavior is dramatically different from GR, we shall immediately set $h^{(0,a)}_{\mu\nu} = 0$ for all a. This choice is justified because we are here interested in CS *deformations* of GR solutions that possess the proper limit that as $\zeta \to 0$, the modified theory

reduces to GR. As such, one cannot allow metric perturbations that modify the flat-space nature of the background in a ζ-independent manner.

III. TEST-PARTICLE MOTION

The first approximation to the dynamics of IMRI/EMRIs is to treat the SCO as a point particle which according to GR follows geodesic motion. In this section we study how this picture is modified in DCSMG, from the change in the geometry of the MBH to the change in the structure of the geodesic equations.

A. MBH geometry

In GR, the geometry of a spinning MBH is described by the Kerr metric, but in the study of CS gravitational modifications it is well known that this is no longer the case [24]. Recently, the corrections to the gravitational field of a spinning black hole have been found [25] in DCSMG using the slow-rotation approximation[2] $a/M \ll 1$ (where M refers to the MBH mass and a is the MBH spin parameter), and the small-coupling approximation up to second order in a/M and ζ. The form of the nonvanishing metric components using coordinates in which the GR part of the metric is Kerr in Boyer-Lindquist coordinates (t, r, θ, ϕ) is

$$\begin{aligned}
\bar{g}_{tt} &= -\left(1 - \frac{2Mr}{\rho^2}\right), \\
\bar{g}_{t\phi} &= -\frac{2Mar}{\rho^2}\sin^2\theta + \frac{5}{8}\frac{\xi}{M^4}\frac{a}{M}\frac{M^5}{r^4}\left(1 + \frac{12M}{7r} + \frac{27M^2}{10r^2}\right) \\
&\quad \times \sin^2\theta, \\
\bar{g}_{rr} &= \frac{\rho^2}{\Delta}, \\
\bar{g}_{\theta\theta} &= \rho^2, \\
\bar{g}_{\phi\phi} &= \frac{\Sigma}{\rho^2}\sin^2\theta,
\end{aligned} \tag{19}$$

where $\rho^2 = r^2 + a^2\cos^2\theta$, $\Delta = r^2 f + a^2$, $f = 1 - 2M/r$ and $\Sigma = (r^2 + a^2)^2 - a^2\Delta\sin^2\theta$. The polar angle θ is not to be confused with the CS scalar field ϑ. Technically, the expressions in Eq. (19) are valid only up to second order in a/M and ζ, but we have here chosen to resum the GR sector, by adding the appropriate high-order uncontrolled remainders. In addition, the expression for the CS scalar field (using the same approximations) is

$$\bar{\vartheta} = \frac{5}{8}\frac{\alpha}{\beta}\frac{a}{M}\frac{\cos(\theta)}{r^2}\left(1 + \frac{2M}{r} + \frac{18M^2}{5r^2}\right). \tag{20}$$

The metric in Eq. (19) is stationary and axisymmetric, and the CS scalar field has the same symmetries. Notice that this CS scalar decays as r^{-2} in the far field and thus it possesses a finite energy.

One could in principle attempt to calculate the $\mathcal{O}[(a/M)^3, \zeta]$ corrections to the metric. These corrections, however, are difficult to find because they involve modifications to all metric components, since the modified field equations must include the scalar stress-energy tensor to this order. We shall not consider these corrections here and work only to leading order with the metric of Eq. (19). Needless to say, if the equivalent metric for rapidly rotating MBHs were found, one could repeat the analysis of this paper for that background spacetime.

The *non-Kerrness* of Eq. (19) allows us to study DCSMG modifications to the multipolar structure of a spinning black hole, as this may illustrate generic corrections of higher-order curvature extensions of GR. The multipolar structure of Kerr is fully determined by *only* two multipole moments: the mass monopole and the current dipole. All others are related to these via the simple relation [77]: $M_\ell + iS_\ell = M(ia)^\ell$, where $\{M_\ell\}_{\ell=0,\ldots,\infty}$ and $\{S_\ell\}_{\ell=0,\ldots,\infty}$ are the mass and current multipole moments, respectively. In DCSMG, the leading-order modification to this relation occurs for the S_4 multipole, as one can see by employing the multipolar formalism of [54] (see also [78]), and noting that the only metric component that is CS modified scales as r^{-4} for $M/r \ll 1$.

DCSMG, therefore, preserves the idea of the no-hair (or two-hair) conjecture that spinning black holes are determined by the mass and spin parameters, but it introduces a 4-pole (or hexadecapole) correction. The reason why DCSMG does not violate the conjecture is because, apart from mass and spin, the other parameters appearing in the MBH metric are introduced through the parameter ξ, which consists of fundamental coupling constants of the theory that are fixed and nontunable (i.e. these constants are analogous to the Newtonian gravitational constant G). Instead, the modifications introduced by DCSMG are such that the standard GR formulas to relate mass and angular momentum to all multipole moments of the solution do not hold.

The high ℓ number of the modification suggests that a GW test of the MBH spacetime geometry (or test of the GR Kerr solution) would require a high accuracy, challenging the abilities of present and future planned detectors. For example, LISA observations are expected to be able to produce accurate measurements of the first 3–5 multipole moments of the MBH (see [79–81] for discussions regarding this problem), which is at the boundary of DCSMG detectability.

B. Motion of massive particles

Let us now consider the equations of motion for massive test particles in DCSMG. The starting point is the action of such a particle moving along a worldline $x^\mu = z^\mu(\lambda)$, where λ parameterizes the trajectory. This action is given

[2] After the publication of this work, other researchers [76] have arrived at the same solution as that presented first in paper I, suggesting a certain robustness and uniqueness of Eq. (19).

by (see e.g. [82])

$$S_{\rm mat} = -m \int_\gamma d\lambda \sqrt{-g_{\alpha\beta}(z)\dot{z}^\alpha \dot{z}^\beta}, \tag{21}$$

where m is the particle mass and $\dot{z}^\mu = dz^\mu/d\lambda$ is the tangent to the worldline γ. The contribution to the matter stress-energy tensor can be obtained by variation of $S_{\rm mat}$ with respect to the metric and yields

$$T^{\alpha\beta}_{\rm mat}(x^\mu) = m \int \frac{d\tau}{\sqrt{-g}} u^\alpha u^\beta \boldsymbol{\delta}^{(4)}[\boldsymbol{x} - \boldsymbol{z}(\tau)], \tag{22}$$

where τ denotes proper time [which is related to λ via $d\tau = d\lambda\sqrt{-g_{\alpha\beta}(z)\dot{z}^\alpha \dot{z}^\beta}$], $u^\mu = dz^\mu/d\tau$ is the particle four-velocity ($g_{\mu\nu}u^\mu u^\nu = -1$), g denotes the metric determinant, and $\boldsymbol{\delta}^{(4)}$ is the four-dimensional Dirac density [$\int d^4x\sqrt{-g}\boldsymbol{\delta}^{(4)}(\boldsymbol{x}) = 1$].

The divergence of $T^{\alpha\beta}_{\rm mat}$ is

$$\nabla_\beta T^{\alpha\beta}_{\rm mat} = m \int \frac{d\tau}{\sqrt{-g}} \frac{d^2 z^\alpha}{d\tau^2} \boldsymbol{\delta}^{(4)}[\boldsymbol{x} - \boldsymbol{z}(\tau)], \tag{23}$$

and, substituting this into the divergence of the field equations [Eq. (4)], we obtain

$$-(\nabla^\nu \vartheta)\left(\beta\Box\vartheta + \frac{\alpha}{4}{}^*RR\right) = m \int \frac{d\tau}{\sqrt{-g}} \frac{d^2 z^\alpha}{d\tau^2} \boldsymbol{\delta}^{(4)}[\boldsymbol{x} - \boldsymbol{z}(\tau)]. \tag{24}$$

Since the left-hand side of this equation vanishes by virtue of the evolution equation [Eq. (5)], all pointlike particles must follow geodesics:

$$\frac{d^2 z^\alpha}{d\tau^2} = 0. \tag{25}$$

Notice that this result is completely generic and does not rely on any approximation scheme.

Let us now consider the structure of the timelike geodesics of the spacetime described by the metric in Eq. (19). Since this metric is a small deformation of the Kerr solution, we can follow the same steps that lead to the derivation of the Kerr geodesic equations in GR (see e.g. [83]) in a form suitable for numerical implementation. The new metric is still stationary and axisymmetric, which means it possesses a timelike Killing vector with components $t^\alpha = [1, 0, 0, 0]$ and a spacelike Killing vector with components $\psi^\alpha = [0, 0, 0, 1]$, respectively. These two Killing vectors commute as in the Kerr case, and we can use them to define two conserved quantities: the energy $E = -t^\alpha u_\alpha$ and the angular momentum $L = \phi^\alpha u_\alpha$. In Boyer-Lindquist coordinates, the particle four-velocity has components $u^\alpha = [\dot{t}, \dot{r}, \dot{\theta}, \dot{\phi}]$, where the overdots now stand for differentiation with respect to proper time τ. We shall work here in reduced variables, where E and L are the energy and angular momentum per unit mass m, respectively.

We can now use the energy and angular momentum definitions to solve for $\dot{t}$ and $\dot{\phi}$. To second order in the slow-rotation approximation, we have

$$\dot{t} = \dot{t}_K + L\delta g^{\rm CS}_\phi, \qquad \dot{\phi} = \dot{\phi}_K - E\delta g^{\rm CS}_\phi, \tag{26}$$

where $\dot{t}_K$ and $\dot{\phi}_K$ denote the corresponding expressions for Kerr:

$$\rho^2 \dot{t}_K = \left[-a(aE\sin^2\theta - L) + (r^2 + a^2)\frac{P}{\Delta}\right], \tag{27}$$

$$\rho^2 \dot{\phi}_K = \left[-\left(aE - \frac{L}{\sin^2\theta}\right) + \frac{aP}{\Delta}\right], \tag{28}$$

and where $P = E(r^2 + a^2) - aL$, while $\delta g^{\rm CS}_\phi$ denotes the CS correction:

$$\delta g^{\rm CS}_\phi = \frac{\alpha^2}{\beta\kappa}\frac{a}{112 r^8 f}(70r^2 + 120rM + 189M^2). \tag{29}$$

As before, we have here resummed the Kerr part of the equations, so that when we take $\alpha \to 0$ we recover the exact equations for the Kerr spacetime for all a, although the expressions presented in this paper are only formally valid up to second order in a/M and ζ.

Following closely the Kerr case, we look for a Killing tensor to construct an additional constant of motion: the Carter constant. We find that such a tensor can be written in the same form as in the Kerr case, namely,

$$\xi_{\alpha\beta} = \Delta k_{(\alpha} l_{\beta)} + r^2 \bar{g}_{\alpha\beta}, \tag{30}$$

where k^α and l^α are two null vectors given by

$$\begin{aligned} k^\alpha &= \left[\frac{r^2 + a^2}{\Delta}, -1, 0, \frac{a}{\Delta} - \delta g^{\rm CS}_\phi\right], \\ l^\alpha &= \left[\frac{r^2 + a^2}{\Delta}, 1, 0, \frac{a}{\Delta} - \delta g^{\rm CS}_\phi\right]; \end{aligned} \tag{31}$$

that is, they are modifications of the Kerr principal null directions. We have checked that they are also principal directions of the new metric up to the order considered here. One can show by direct evaluation that this tensor satisfies the tensor Killing equations $\nabla_{(\rho}\xi_{\alpha\beta)} = 0$ on the CS modified Kerr background if and only if $\delta g^{\rm CS}_\phi$ is given by Eq. (29). In fact, the tensor Killing equations allow us to add a term of the form C/r^2 to Eq. (29), but the orthogonality relation $k^\alpha l_\alpha = 0$ forces $C = 0$.

We can now define the Carter constant in the same way as in the Kerr case:

$$\mathcal{Q} = \xi_{\alpha\beta}u^\alpha u^\beta - (L - aE)^2. \tag{32}$$

Using this relation, together with Eqs. (27) and (28) and the normalization condition for timelike geodesics $g_{\alpha\beta}u^\alpha u^\beta = -1$, we can solve for $\dot{r}$ and $\dot{\theta}$. We find that the result can be written as

$$\dot{r}^2 = \dot{r}_K^2 + 2ELf\delta g_\phi^{\rm CS}, \qquad \dot{\theta}^2 = \dot{\theta}_K^2, \tag{33}$$

where the part that corresponds to Kerr (without expanding in a/M) is

$$\rho^4 \dot{r}_K^2 = [(r^2 + a^2)E - aL]^2 - \Delta[Q + (aE - L)^2 + r^2], \tag{34}$$

$$\rho^4 \dot{\theta}_K^2 = Q - \cot^2\theta L^2 - a^2\cos^2\theta(1 - E^2). \tag{35}$$

To summarize, Eqs. (26) and (33) provide a set of four first-order (in derivatives of τ) decoupled geodesic equations for the CS modified Kerr background. We note that these geodesic equations contain CS corrections except for the $\dot{\theta}$ equation, and that these corrections have essentially the same structure, in the sense that all of them are proportional to $\delta g_\phi^{\rm CS}$ [Eq. (29)]. We remind the reader once more that the polar angle θ and its evolution equation $\dot{\theta}$ are not to be confused with the CS scalar field ϑ and its time derivative $\dot{\vartheta}$.

One can easily show that the location of the innermost stable circular orbit (ISCO) for equatorial orbits in the CS modified metric is given by [25]

$$R_{\rm ISCO} = 6M \mp \frac{4\sqrt{6}a}{3} - \frac{7a^2}{18M} \pm \frac{77\sqrt{6}a}{5184}\frac{\alpha^2}{\beta\kappa M^4}, \tag{36}$$

where the upper (lower) signs correspond to corotating (counterrotating) geodesics. Then, it appears that the CS correction works against the spin effects, which suggests that similar behavior will be present in the solution of the CS modified geodesic equations.

C. Frequencies of the orbital motion

The Kerr metric allows bound and stable geodesic trajectories (orbits) to be associated or decomposed in terms of three *fundamental* frequencies (see e.g. [84,85]): Ω_r characterizes the radial motion (from periapsis to apoapsis and back); Ω_θ characterizes the motion in the polar direction; and Ω_ϕ characterizes azimuthal motion. These frequencies are important because precessional orbital effects are due to mismatches among them and because they can be used to decompose, among other things, the gravitational waveform in a Fourier expansion.

Expressions for these frequencies in terms of quadratures have been obtained for Kerr in [84], and recently also in [85], where a new time coordinate is employed (see [47]): $\rho^2 d/d\tau = d/d\lambda$. In terms of the time λ, the modified geodesic equations become

$$\frac{dt}{d\lambda} = T_K(r,\theta) + T_{\rm CS}(r), \qquad \left(\frac{dr}{d\lambda}\right)^2 = R_K(r) + R_{\rm CS}(r),$$
$$\frac{d\phi}{d\lambda} = \Phi_K(r,\theta) + \Phi_{\rm CS}(r), \qquad \left(\frac{d\theta}{d\lambda}\right)^2 = \Theta_K(\theta), \tag{37}$$

where $(T_K, R_K, \Theta_K, \Phi_K)$ are given by the right-hand sides of Eqs. (27), (28), (34), and (35), respectively, while $(T_{\rm CS}, R_{\rm CS}, \Phi_{\rm CS})$ are quantities proportional to $\delta g_\phi^{\rm CS}$. Note that the CS corrections only depend on r, which is a consequence of the linearization in a/M.

The fundamental frequencies of the radial and polar motions associated with the λ time are

$$\mathcal{Y}_r = \frac{2\pi}{\Lambda_r} \sim \frac{2\pi}{\Lambda_r^K}\left(1 - \frac{\Lambda_r^{\rm CS}}{\Lambda_r^K}\right), \qquad \mathcal{Y}_\theta = \frac{2\pi}{\Lambda_\theta} = \frac{2\pi}{\Lambda_\theta^K}, \tag{38}$$

where the periods, denoted by Λ, are given by

$$\Lambda_r^K = 2\int_{r_{\rm peri}}^{r_{\rm apo}} \frac{dr}{\sqrt{R_K}}, \qquad \Lambda_r^{\rm CS} = -\int_{r_{\rm peri}}^{r_{\rm apo}} dr \frac{R_{\rm CS}}{R_K^{3/2}}, \tag{39}$$

$$\Lambda_\theta^K = 2\int_{\theta_{\rm min}}^{\pi-\theta_{\rm min}} \frac{d\theta}{\sqrt{\Theta_K}} = 4\int_{\theta_{\rm min}}^{\pi/2} \frac{d\theta}{\sqrt{\Theta_K}}, \tag{40}$$

where $r_{\rm apo}$ and $r_{\rm peri}$ are the apocenter and pericenter values of r, respectively, and $\theta_{\rm min}$ determines the interval in which θ oscillates, i.e. $(\theta_{\rm min}, \pi - \theta_{\rm min})$. The frequency associated with the azimuthal motion is given by [85]

$$\mathcal{Y}_\phi = \frac{1}{(2\pi)^2}\int_0^{2\pi} dw^r \int_0^{2\pi} dw^\theta \Phi[r(w^r), \theta(w^\theta)], \tag{41}$$

where $w^{r,\theta} = \mathcal{Y}_{r,\theta}\lambda$ are the associated angle variables. Therefore, only $\mathcal{Y}_r$ and $\mathcal{Y}_\phi$ change with respect to GR.

The expressions for the fundamental frequencies with respect to the coordinate time t, $\Omega_{r,\theta,\phi}$ are more involved since they are given by $\Omega_{r,\theta,\phi} = \mathcal{Y}_{r,\theta,\phi}/\Gamma$, and Γ is [85]

$$\Gamma = \frac{1}{(2\pi)^2}\int_0^{2\pi} dw^r \int_0^{2\pi} dw^\theta T[r(w^r), \theta(w^\theta)]. \tag{42}$$

Inverting this relation cannot be easily done in close form, without previously solving the integrals numerically (see e.g. [84] for an analytical inversion in terms of incomplete elliptical integrals). We immediately see, however, that since T is CS corrected, so will be Γ, leading to CS corrections in all the frequencies associated with the coordinate time t.

Since the three physical fundamental frequencies of the Kerr spacetime are modified in CS modified gravity, given a detection of quasinormal modes from a Kerr-like object, the inference of system parameter could lead to a systematic error due to the bias of assuming GR is the correct underlying theory [86]. Conversely, the detection of such modes with LISA may yield an interesting constraint on dynamical CS modified gravity.

IV. GRAVITATIONAL-WAVE GENERATION AND THE SEMIRELATIVISTIC APPROXIMATION

In this section we look at the structure of the modified field equations of DCSMG to study how gravitational-wave generation formulas change with respect to the GR ones. We also describe the semirelativistic approximation

for the description of IMRI/EMRI systems and the details of the implementation that we use in this paper.

A. GW generation in DCSMG

Taking into account the extreme-mass ratios involved, the systems under consideration can be well described using perturbation theory around the background quantities given in Sec. III A. In that section, we showed that these background quantities contain a GR contribution plus perturbations in the CS coupling parameter ζ and in the black hole rotation parameter a/M. Similarly, here we shall expand the perturbations generated by the SCO (treated here as a particle) orbiting the MBH also in powers of a third parameter: the mass ratio of the system $\mu = m/M$.

Neglecting the slow-rotation approximation for the time being, the metric and the CS scalar field can be expanded as follows:

$$\begin{aligned} \mathrm{g}_{\mu\nu} &= \bar{\mathrm{g}}_{\mu\nu} + \sum_{n=1,m=0} \mu^n \zeta^m h^{(n,m)}_{\mu\nu} \\ &= \bar{\mathrm{g}}_{\mu\nu} + \mu h^{(1,0)}_{\mu\nu} + \mu\zeta h^{(1,1)}_{\mu\nu} + \cdots, \end{aligned} \tag{43}$$

$$\begin{aligned} \vartheta &= \bar{\vartheta} + \sum_{n=1,m=0} \mu^n \zeta^m \vartheta^{(n,m)} \\ &= \bar{\vartheta} + \mu\vartheta^{(1,0)} + \mu\zeta\vartheta^{(1,1)} + \cdots, \end{aligned} \tag{44}$$

where $(\bar{\mathrm{g}}_{\mu\nu}, \bar{\vartheta})$ are given in Eqs. (19) and (20) and $h^{(n,m)}_{\mu\nu}$ and $\vartheta^{(n,m)}$ now stand for the perturbations of $\mathcal{O}(\mu^n, \zeta^m)$ (alternatively, one can think of μ as playing the role of ϵ in Sec. II D).

The equation for the metric perturbation $h^{(1,0)}_{\mu\nu}$, in the Lorenz gauge [Eq. (9)], is

$$\mu\{\bar{\Box} h^{(1,0)}_{\mu\nu} + 2\bar{R}^{\rho}{}_{\mu}{}^{\sigma}{}_{\nu} h^{(1,0)}_{\rho\sigma}\} = -\frac{1}{\kappa} T^{\mathrm{mat}}_{\mu\nu}, \tag{45}$$

where there are no contributions from the CS scalar field at this order of approximation, and thus, this is a purely GR GW generation equation. Similarly, the equation for $\vartheta^{(1,0)}$ is

$$\begin{aligned} \bar{\Box}\vartheta^{(1,0)} &= h^{(1,0)\mu\nu}\bar{\nabla}_{\mu}\bar{\nabla}_{\nu}\bar{\vartheta} + \bar{\mathrm{g}}^{\mu\nu(1)}\Gamma^{\rho}_{\mu\nu}\bar{\nabla}_{\rho}\bar{\vartheta} \\ &\quad - \frac{\alpha}{4\beta}{}^{(1)}({}^{*}RR), \end{aligned} \tag{46}$$

where ${}^{(1)}\Gamma^{\rho}_{\mu\nu}$ and ${}^{(1)}({}^{*}RR)$ denote the first-order perturbations of the Christoffel symbols and the Pontryagin density, respectively, about $\bar{\mathrm{g}}_{\mu\nu}$ and evaluated at $h^{(1,0)}_{\mu\nu}$. That is, $\vartheta^{(1,0)}$ is generated by the metric perturbations $h^{(1,0)}_{\mu\nu}$ which, in turn, are generated by the motion of the SCO around the MBH. The first two terms on the right-hand side of Eq. (46) are proportional to the spin parameter a/M. This is not the case for the third term, since this is nonzero for a Schwarzschild BH [23], which implies that $\vartheta^{(1,0)}$ will contain terms proportional to a but also terms that are a-independent.

The next correction to the metric perturbations in the small-coupling approximation is $h^{(1,1)}_{\mu\nu}$, which satisfies an equation with the following structure:

$$\begin{aligned} &\zeta\{\bar{\Box} h^{(1,1)}_{\mu\nu} + 2\bar{R}^{\rho}{}_{\mu}{}^{\sigma}{}_{\nu} h^{(1,1)}_{\rho\sigma}\} \\ &= \frac{2\alpha}{\kappa}\{C_{\mu\nu}[\vartheta^{(1,0)}, \bar{\mathrm{g}}_{\rho\sigma}] + {}^{(1)}C_{\mu\nu}[\bar{\vartheta}, h^{(1,0)}_{\mu\nu}]\} \\ &\quad - 2\frac{\beta}{\kappa}\Big\{\bar{\nabla}_{(\mu}\bar{\vartheta}\bar{\nabla}_{\nu)}\vartheta^{(1,0)} - \frac{1}{2}\bar{\mathrm{g}}_{\mu\nu}\bar{\nabla}^{\sigma}\bar{\vartheta}\bar{\nabla}_{\sigma}\vartheta^{(1,0)} \\ &\quad - \frac{1}{4}h^{(1,0)}_{\mu\nu}\bar{\nabla}^{\sigma}\bar{\vartheta}\bar{\nabla}_{\sigma}\bar{\vartheta}\Big\}, \end{aligned} \tag{47}$$

where ${}^{(1)}C_{\mu\nu}$ is the first-order perturbation of the C tensor when only the metric is perturbed [see Appendix B 1 for explicit formulas of these quantities]. Note that the terms on the right-hand side of Eq. (47) depend only on the background (overbarred) quantities and the $(1, 0)$ perturbations, which are determined by Eqs. (45) and (46).

The leading-order CS correction to the GW generation formalism is then determined by Eq. (47), so let us now analyze its structure. The first term in this equation is $(2\alpha/\kappa)C_{\mu\nu}[\vartheta^{(1,0)}, \bar{\mathrm{g}}_{\rho\sigma}]$, and it contains two pieces:

$$(2\alpha/\kappa)(\bar{\nabla}_{\sigma}\vartheta^{(1,0)})\bar{\epsilon}^{\sigma\delta\alpha(\mu}\bar{\nabla}_{\alpha}\bar{R}^{\nu)}{}_{\delta}, \tag{48}$$

$$(2\alpha/\kappa)(\bar{\nabla}_{\sigma}\bar{\nabla}_{\delta}\vartheta^{(1,0)})^{*}\bar{R}^{\delta(\mu\nu)\sigma}. \tag{49}$$

Since the background is Kerr plus terms of order ζ, Eq. (48) is actually at least of $\mathcal{O}(\zeta^2\mu a/M)$, and we can then ignore it to compute $h^{(1,1)}_{\mu\nu}$. The second piece [Eq. (49)] is actually the only one in Eq. (47) that is not proportional to the spin parameter, making it of $\mathcal{O}(\zeta\mu)$, since the dual to the Riemann of the Schwarzschild metric is nonvanishing. The last term in Eq. (47) is at least quadratic in a/M, making it of $\mathcal{O}(\zeta\mu a^2/M^2)$, since $\bar{\vartheta}$ is linear in the spin parameter. All remaining terms are at least linear in the spin parameter and of $\mathcal{O}(\zeta\mu a/M)$, since they are all proportional to derivatives of $\bar{\vartheta}$, which in turn is proportional to a/M [see Eq. (20)].

The structure of Eq. (47) thus reveals that if one were to employ the slow-rotation approximation, as in the computation of the MBH metric [25] (see Sec. III A), the leading-order evolution equation for the metric perturbation becomes

$$\zeta\{\bar{\Box} h^{(1,1)}_{\mu\nu} + 2\bar{R}^{\rho}{}_{\mu}{}^{\sigma}{}_{\nu} h^{(1,1)}_{\rho\sigma}\} = \frac{2\alpha}{\kappa}(\bar{\nabla}_{\sigma}\bar{\nabla}_{\delta}\vartheta^{(1,0)})^{*}\bar{R}^{\delta(\mu\nu)\sigma}. \tag{50}$$

Once this equation is solved for $h^{(1,1)}_{\mu\nu}$, one could use it to solve the evolution equation for $\vartheta^{(1,1)}$, which we have not presented here. In this way, one could proceed with the bootstrapping method described in [25] and in Sec. II B to

build higher-order perturbations in the metric and the CS scalar field.

In summary, GW emission in DCSMG is determined by the following equations. To first order, the metric perturbation is generated by the SCO through the GR relation in Eq. (45), leading to $h^{(1,0)}_{\mu\nu} = \mathcal{O}(\mu)$. To second order, the metric perturbation contains two contributions: a term $h^{(2,0)}_{\mu\nu} = \mathcal{O}(\mu^2)$ and a CS modification to the first-order term $h^{(1,1)}_{\mu\nu} = \mathcal{O}(\mu\zeta)$. The latter can be obtained by solving Eq. (50), which requires knowledge of the leading-order perturbation to the CS scalar due to the SCO, $\vartheta^{(1,0)}$, which in turn is determined by Eq. (46) once one has solved for $h^{(1,0)}_{\mu\nu}$ through Eq. (45). In this paper we shall only employ the first-order terms $h^{(1,0)}_{\mu\nu}$ to model GWs, and thus modifications to the waveforms arise exclusively due to corrections to the trajectories.

A proper treatment of the EMRI problem would also require the use of the first-order perturbations to estimate backreaction, self-force effects on the SCO trajectory (see e.g. [82]), which involves calculations that have *not* been carried out in full generality even in pure GR. Only through the adiabatic approximation have there been studies of such backreaction for spinning MBHs [43–52], where one assumes that only GW dissipation is important. The purpose of this paper, however, is to elucidate the main differences between GR and DCSMG dynamics for IMRI/EMRI systems, and thus, calculations with backreaction are far too complex. Instead, we will resort to the so-called semirelativistic approximation, which we describe in the next subsection.

B. The semirelativistic approximation

First introduced by Ruffini and Sasaki [53], this approximation makes two critical assumptions to simply the modeling of GW generation: (i) the SCO moves along geodesics of the MBH background geometry; (ii) the SCO emits GWs as if it were moving in flat space. Assumption (i) is justified on the basis that for EMRIs the more extreme the mass ratio, the closer one is to the point-particle limit, and hence the closer the motion is to geodesic. Assumption (ii) is useful because it allows us to neglect the curvature of the background in the generation and propagation of GWs from the SCO to the observer in the radiation zone. Such usefulness, however, is not a justification; a justification for assumption (ii) arises only after one compares GWs computed in the semirelativistic approximation versus GWs generated in more exact prescriptions.

Recently, the assumptions the semirelativistic approximation is based upon have been shown to be justified in that they provide an accurate approximation to GWs generated by more precise methods. Babak *et al.* [58] have shown that semirelativisticlike calculations can lead to waveforms with high overlaps with Teukolsky-based waveforms, where for the latter the GW fluxes for the adiabatic approximation are calculated from solutions to the Teukolsky equation for perturbations of a Kerr background. Babak *et al.*[58] also describe how to incorporate radiation reaction in the calculations by using certain post-Newtonian prescriptions, and compare fluxes of energy and angular momentum with Teukolsky-based estimations. Such comparisons suggest that post-Newtonian prescription of radiation reaction also seem to lead to waveforms that capture most of the essential features of the Teukolsky-based simulations.

Following the work of Ruffini and Sasaki [53], the implementation of the semirelativistic approximation is as follows. Once the geodesic equations have been solved for the orbital trajectories, the metric perturbation is obtained from Eq. (45), but assuming that the background metric $\bar{g}_{\mu\nu}$ is the flat spacetime metric. In this way, the solution to the perturbative equation is given by the gravitational Lienard-Wiechert potentials (see e.g. [87,88] for the derivation of the electromagnetic version of these potentials), which contain all the information necessary to reconstruct the gravitational field generated by the SCO.

In this paper, we shall employ a formulation of the semirelativistic approximation in which the first assumption (geodesic motion with respect to the MBH background geometry) is still employed, but the second one is slightly modified. More precisely, we shall still assume that GWs are emitted as if in flat space but, following [58,89], we solve the perturbative equations using a multipolar expansion, which is determined by the source multipole moments and which is valid for objects with arbitrarily strong internal gravity (see [54] for a detailed discussion of these expansions).

The multipolar treatment of gravitational radiation is truly a slow-motion approximation as the series is truncated at a finite multipole order. For a compact-body binary system, the error scales with a high power of the orbital velocity, which for EMRIs can typically be larger than half the speed of light, and may lead to the loss of certain relativistic features in the waveforms (see e.g. [90] in the context of post-Newtonian theory and EMRIs). In spite of these drawbacks, the semirelativistic approximation has been shown to capture the correct qualitative behavior of EMRI orbits and waveforms, and thus, it will suffice to present the main features of the CS modifications to GW generation.

Another possibility to estimate the GW emission is to use the weak-gravity/fast-motion formula derived by Press [91], whose implementation requires the same information as the multipolar formula truncated after the mass octopole and current quadrupole. This formula has been used in [58], where it has been shown to provide accurate results as compared to Teukolsky-based waveforms. We shall not employ this formalism here, however, choosing to work instead with the standard multipolar decomposition.

We have shown that up to order $\mathcal{O}(\mu\zeta)$ the perturbative GW generation equations for IMRI/EMRI systems have the same form as in GR. Any difference in the waveforms will then arise due to differences in the geodesic equations due to the modified Kerr background. In the transverse-traceless (TT) gauge, defined by Eqs. (9) and (10) and in which the dynamical degrees of freedom have been isolated, the metric perturbations describing the GWs emitted by an isolated system are given by [54]

$$h_{ij}^{\mathrm{TT}} = \Bigg[\sum_{\ell=2}^{\infty} \frac{4}{\ell! r} I^{(\ell)}_{ijA_{\ell-2}}(t_{\mathrm{ret}}) N_{A_{\ell-2}} + \sum_{\ell=2}^{\infty} \frac{8\ell}{(\ell+1)! r} \varepsilon_{kl(i} J^{(\ell)}_{j)kA_{\ell-2}}(t_{\mathrm{ret}}) n_l N_{pA_{\ell-2}} \Bigg]^{\mathrm{TT}}, \quad (51)$$

where we have adopted the multi-index notation of [54]: A_ℓ is a multi-index (sequence of ℓ indices: $a_1 \ldots a_\ell$) so that $N_{A_\ell} = n_{a_1} \ldots n_{a_\ell}$ is the product of ℓ unit vectors $n^i = x^i/r$ that point in the direction from the source toward the observer, with $r = (\delta_{ij} x^i x^j)^{1/2}$ the flat-space distance from the source to the observer; there is summation over repeated indices independently of their location; ε_{ijk} is the three-dimensional flat-space Levi-Civita tensor.

The mass and current multipole moments of the source, I_{A_ℓ} and J_{A_ℓ}, respectively, are given by [54]

$$I_{A_\ell} = \Bigg[\int d^3x \rho x_{A_\ell}\Bigg]^{\mathrm{STF}}, \qquad J_{A_\ell} = \Bigg[\int d^3x \rho (\varepsilon_{a_\ell jk} x_i v_k) x_{A_{\ell-1}}\Bigg]^{\mathrm{STF}}, \quad (52)$$

where $x_{A_\ell} = x_{a_1} \ldots x_{a_\ell}$ and ρ is the mass density of the source, which in our case corresponds to the mass density of the SCO, given by

$$\rho(t, x^i) = m \boldsymbol{\delta}^{(3)}[x^i - z^i(t)], \quad (53)$$

where $\boldsymbol{\delta}^{(3)}$ denotes the Dirac-delta distribution, $z^i(t)$ is the spatial trajectory of the SCO, and $v^i = dz^i/dt$ is its spatial velocity with respect to the coordinate time t. In Eq. (51) the mass and current multipole moments have to be evaluated at the retarded time $t_{\mathrm{ret}} = t - r$ and the superscript (ℓ) denotes their ℓth time derivative.

The projectors STF in Eqs. (52) and TT in Eq. (51) are symmetric/trace-free and transverse/traceless operators, respectively. The latter is obtained by means of the projector orthogonal to n^i, namely, $P^i_j = \delta^i_j - n^i n_j$, in the following way:

$$[A_{ij}]^{\mathrm{TT}} = P^k_i P^l_j A_{kl} - \tfrac{1}{2} P_{ij} P^{kl} A_{kl}. \quad (54)$$

An orthonormal triad $\{n^i, p^i, q^i\}$, with respect to the spatial flat-space metric and associated with n^i, can always be constructed to build the polarization tensors via $\varepsilon^+_{ij} = p_i p_j - q_i q_j$ and $\varepsilon^\times_{ij} = 2 p_{(i} q_{j)}$.

With these tensor projectors and Eq. (51) we can obtain the two independent GW polarizations as follows:

$$h_+ = \tfrac{1}{2} \varepsilon^{+ij} h^{\mathrm{TT}}_{ij}, \qquad h_\times = \tfrac{1}{2} \varepsilon^{\times ij} h^{\mathrm{TT}}_{ij}, \quad (55)$$

or equivalently

$$h^{\mathrm{TT}}_{ij} = h_+ \varepsilon^+_{ij} + h_\times \varepsilon^\times_{ij}. \quad (56)$$

In this paper we use this multipolar decomposition to compute the GW emission including terms up to the mass octopole and current quadrupole moment.

Another important question for the implementation of this version of the semirelativistic approximation is the choice of coordinates. More specifically, the equations of motion (geodesics) are written in Boyer-Lindquist coordinates (see Sec. III B), whereas the formulas given in this section require Cartesian coordinates. Thus, one must decide how to construct Cartesian coordinates that cover the motion of the SCO and at the same time the observer in the radiation zone. One possibility would be to rewrite the background MBH metric and the equations of motion in Cartesian-like coordinates such that at infinity the metric becomes the flat spacetime metric in Cartesian coordinates. This choice was made in [89] for the study of extreme-mass-ratio gravitational-wave bursts. A different choice is to identify Boyer-Lindquist coordinates (r, θ, ϕ) with flat-space spherical coordinates and then introduce Cartesian coordinates through the familiar relations

$$x = r \sin\theta \cos\phi, \qquad y = r \sin\theta \sin\phi, \qquad z = r \cos\theta. \quad (57)$$

This was the choice made in [58] for the construction of EMRI *kludge* waveforms. Numerical experiments [92] show that indeed different choices of Cartesian coordinates produce different waveforms. However, differences are significant only for relativistic orbits, and for those, these differences appear dominantly in the amplitudes but not in the phase. In this paper we shall employ the second choice of Cartesian coordinates for the computation of the gravitational waveforms.

V. GRAVITATIONAL WAVES FROM IMRI/EMRI SYSTEMS IN DCSMG

In this section we study numerically the evolution of IMRI/EMRIs and their GW emission in the semirelativistic approximation and in the context of the DCSMG theory. We describe the numerical implementation and apply it to a number of test systems, presenting the trajectories and the waveforms associated with them.

A. Numerical evolution and test systems

In the semirelativistic approximation the numerical calculations can be divided into two stages: first, the computation of the SCO trajectory around the MBH and, second,

the computation of the gravitational waveforms given the trajectory. The starting point for the computation of the trajectory, namely, $[t(\tau), r(\tau), \theta(\tau), \phi(\tau)]$ are the geodesic equations [Eqs. (26) and (33)]. Clearly, when the CS parameter ξ is small the dynamics will be close to GR. Since there are already bounds on this parameter from binary pulsar tests [25], albeit weak, we shall be here interested only in small CS deformation of GR EMRI/IMRI waveforms.

As in GR, for bound orbits the equations for $r(\tau)$ and $\theta(\tau)$ present turning points which are difficult to treat numerically. This can be avoided by introducing the following alternative variables (see e.g. [85] for details):

$$r = \frac{pM}{1 + e\cos\psi}, \qquad \cos^2\theta = \cos^2(\theta_{\rm min})\cos^2(\chi), \quad (58)$$

where p is the *semilatus rectum*, e is the eccentricity, and as we mentioned before $\theta \in (\theta_{\rm min}, \pi - \theta_{\rm min})$. The geodesic equations then become evolution equations for the variables (ψ, χ, ϕ) with respect to Boyer-Lindquist time t, where one uses the $dt/d\tau$ equation [Eq. (26)] to transform from proper to coordinate time. The form of the ordinary differential equations (ODEs) for $[\psi(t), \chi(t), \phi(t)]$ in GR can be found from the developments presented, for instance, in [85].

From a numerical standpoint, ODE solvers for $[\psi(t), \chi(t), \phi(t)]$ require knowledge of the turning points, which will be here CS modified. In particular, the radial turning points are modified, since the ODE for $\psi(t)$ is corrected by new CS terms that arise in the $dr/d\tau$ equation. In contrast, the polar turning points are not modified, since these arise from the $d\theta/d\tau$ equation, which is not CS corrected. All of this suggests that prescribing a set of initial constants of motion (E, L, Q) leads to three orbital parameters (p, e, ι), which are not identical to the ones that one would obtain in GR.

Let us define these orbital parameters more carefully, since they play an important role in our calculations. The semilatus rectum and the eccentricity parameter, p and e, respectively, are defined such that the apocenter $r_{\rm apo}$ and pericenter $r_{\rm peri}$ (two of the turning points of the equation for $dr/d\tau$) have the familiar Newtonian expression

$$r_{\rm apo} = \frac{pM}{1 - e}, \qquad r_{\rm peri} = \frac{pM}{1 + e}. \quad (59)$$

The third orbital parameter, the orbital inclination with respect to the equatorial plane ι, is defined as $\tan\iota = Q/L$, but it is sometimes more convenient to describe it in terms of the angle $\theta_{\rm inc} = \pi/2 - {\rm sgn}(L)\theta_{\rm min}$, which is directly related to the turning points of $\theta(\tau)$. Clearly, the functional form of $(p, e, \theta_{\rm inc})$ in terms of (E, L, Q) differs in GR and in DCSMG, and thus, if one prescribes a set of constants of motion (E_0, L_0, Q_0) in GR, the resultant orbit will not possess the same orbital parameter as its DCSMG counterpart. In the results presented below, we compare trajectories that have the *same* orbital parameters, $(p, e, \theta_{\rm inc})$, instead of comparing trajectories with the same constants of motion (E, L, Q).

Regarding the numerical integration of the ODEs for $[\psi(t), \chi(t), \phi(t)]$, we use the Bulirsch-Stoer extrapolation method [93] as the evolution algorithm (details on this method and its implementation can be found in [94,95]). Our numerical code is complemented with a number of routines to construct Boyer-Lindquist and Cartesian-like coordinates and their associated time derivatives.

Waveforms are computed with the multipolar expansion of Sec. IV B, up to the mass octupole and current quadrupole, which requires as input the trajectory $x^i(t)$, the spatial velocity $v^i(t)$, the spatial acceleration $a^i(t)$, and its time derivative, the *jerk*, $j^i(t) = da^i(t)/dt$. These time derivatives are computed using a finite differences differentiation rule with nine points. The error in the computation of the jerk scales with the time step Δt as $(\Delta t)^8$, well within the accuracy range that we need for our calculations.

We have here evolved the geodesic equations for a total time of $T = 5 \times 10^5 M$, obtaining on the order of 10^3–10^4 cycles. The type of geodesic is prescribed in terms of the following orbital parameters: the pericenter *distance* $r_{\rm peri}$, the eccentricity e, and the inclination angle $\theta_{\rm inc}$. We implemented a double-bisection algorithm to guarantee that the turning points in both the GR evolutions and the DCSMG ones correspond to orbits with the same orbital parameters $(p, e, \theta_{\rm inc})$, up to an accuracy of one part in 10^{14}.

The MBH background metric of Eq. (19) is fully determined by the choice of the mass M and spin parameter $a = J/M$, where J is the spin angular momentum, plus the ratio ξ. The SCO is characterized by its mass m, which then also defines the mass ratio $\mu = m/M$. As we have mentioned, the type of orbit is fully determined by the choice of orbital parameters $(r_{\rm peri}, e, \theta_{\rm inc})$, while we still need to fully determine the initial conditions of the motion by prescribing $(\psi_o, \chi_o, \phi_o) = (\psi(t_o), \chi(t_o), \phi(t_o))$, where t_o is the initial time for the numerical evolution of our system of ODEs. We shall here always set $\beta = \alpha$, $M = M_\bullet$, where $M_\bullet = 4.5 \times 10^6 M_\odot$ is approximately the mass of the presumable MBH at the center of the Milky Way [96]. For the mass of the SCO we choose $m = 35 M_\odot$, which leads to the following mass ratio: $\mu \sim 7.8 \times 10^{-6}$.

The particular *test* systems that we consider in this paper are defined as follows:

(A) $a = 0.1M$ and $\xi = 0.1M^4$, with orbital parameters $(r_{\rm peri}, e, \theta_{\rm inc}) = (12M, 0.2, 0.1)$,

(B) $a = 0.2M$ and $\xi = 0.2M^4$, with orbital parameters $(r_{\rm peri}, e, \theta_{\rm inc}) = (8M, 0.4, 0.2)$,

(C) $a = 0.4M$ and $\xi = 0.4M^4$, with orbital parameters $(r_{\rm peri}, e, \theta_{\rm inc}) = (6M, 0.6, 0.3)$,

while the waveforms are measured by observers located on the z axis at a distance of approximately 8 kpc (roughly the

distance from the Solar System to the center of our Galaxy). Clearly, the test systems have been ordered from the least relativistic to the most relativistic. We are forced to choose a and ζ such that the slow-rotation approximation $a/M \ll 1$ and the small-coupling approximation $\zeta \ll 1$ used for constructing the MBH background [25] are satisfied. In this sense, the error in the MBH background metric scales as $\zeta(a^3/M^3)$, which for systems (A), (B), and (C) implies errors in the MBH background of $\mathcal{O}(10^{-4})$, $\mathcal{O}(10^{-3})$, and $\mathcal{O}(10^{-2})$, respectively, relative to the true DCSMG waveforms for an exact, spinning MBH background. One might worry that the coefficient in front of these order symbols might be large, but as one can see in Eqs. (29) and (36), the coefficient in front of the correction to the location of the ISCO is of $\mathcal{O}(10^{-3})$, while the largest coefficient of the modification to the geodesic equation is $\mathcal{O}(10^{-5})$ at pericenter for system (C).

B. Orbital trajectories

The test systems described above present rather similar orbital behavior. Generically, there is a stage of zoom-whirl, where the particle spends several cycles close to the pericenter radius $r_{\rm peri}$ followed by a stage where it orbits at a larger radius r, close to $r_{\rm apo}$. Moreover, there is generically both in-plane and out-of-the-plane precession. The orbit produced by test system (B) in GR is shown in Fig. 2, where we have plotted only the last time interval of duration $17\,500M$ of the geodesic evolution. From this figure we can observe the generic Lense-Thirring precession as well as the two stages described above.

The CS correction to the background has a clear effect on the trajectories of the bodies. Figure 3 plots the projection of the orbital trajectories for system (C) onto the x-y plane for the CS background (black line) and the Kerr background (light gray line) and the last $17\,500M$ of the geodesic evolution. Notice that the orbital trajectories have dephased significantly by the end of the evolution.

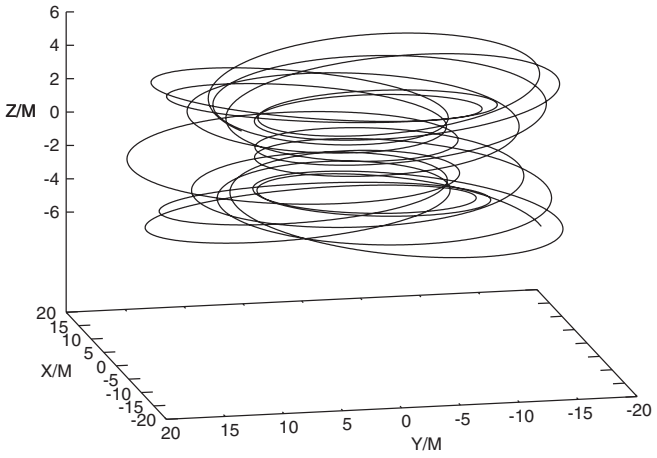

FIG. 2. Three-dimensional depiction of the last cycles of system (B) before the evolution was stopped.

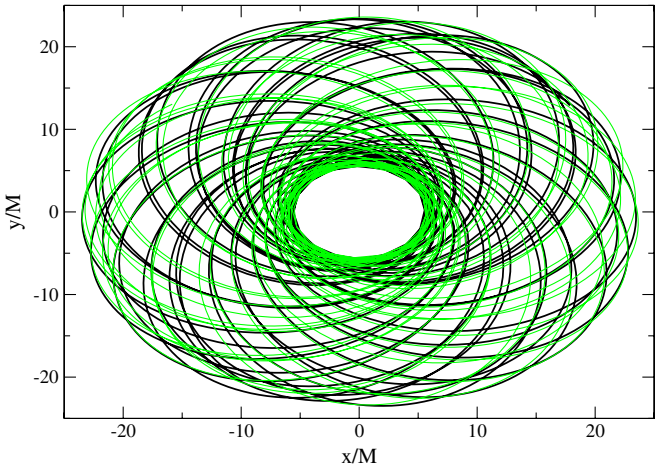

FIG. 3 (color online). Two-dimensional projection onto the x-y plane of system (C)'s orbital trajectories in a Kerr background (light gray lines) and in the CS corrected Kerr solution (black lines).

From this figure one cannot discern whether the CS trajectories trail or anticipate the GR ones, but this can be assessed by plotting the difference between the GR and CS evolved angles (ψ, χ, ϕ) that determine completely the geodesic evolution. These angles are the Boyer-Lindquist azimuthal angle ϕ plus the two angles ψ and χ associated with the other Boyer-Lindquist coordinates r and θ through the relations in Eq. (58). Figure 4 plots the dephasing in ψ, where we observe that, in all panels, the difference $\delta\psi := \psi_{\rm CS} - \psi_{\rm GR}$ is initially close to zero and then it decreases linearly on average (over a number of cycles). Also we observe that, as expected, system (C) presents the biggest dephasing, followed by system (B) and then by system (A) (note the change of scale in the y axis). Similar linear dephasing trends are observed in $\delta\chi$ and $\delta\phi$.

For weakly gravitating systems, we find that $\delta\psi$ is dominant and negative, while $\delta\chi \sim -\delta\phi$, with the latter

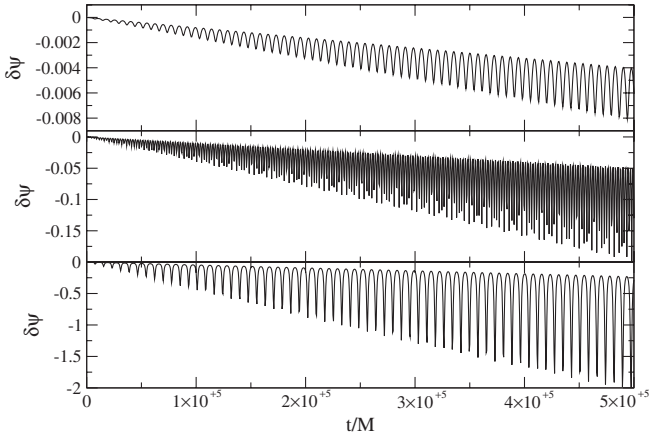

FIG. 4. Dephasing of the ψ coordinate as a function of time. The top panel corresponds to system (A), the middle one to system (B) and the bottom one to system (C).

positive. This implies that the CS orbits of systems (A) and (B) are overall trailing the GR solution. This scenario is a bit more complicated for system (C), where $\delta\psi \ll 0$ is still dominant, but both $\delta\phi$ and $\delta\chi$ are positive, implying that the CS orbits still trail the GR one in radius, but anticipate it in angles θ and ϕ.

C. Gravitational waveform

Orbital trajectories can give us a sense of the CS effect on geodesics, but the true observables are gravitational waveforms. Figure 5 plots the difference in the waveforms computed with CS trajectories and GR trajectories. For reference, the maximum magnitude of the GR GW polarization h_+ is approximately $|h_+| < 8 \times 10^{-17}$ [system (A)], $|h_+| < 1.25 \times 10^{-16}$ [system (B)], and $|h_+| < 2.25 \times 10^{-16}$ [system (C)]. At the end of the simulation (~ 128 days of data using $M = M_\bullet$), we observe that system (A) has dephased by as much as 0.3%, while system (B) has dephased by 16%, and system (C) by 90% relative to the maximum amplitude of the respective GR waveforms. Similar behavior is observed for the other polarization.

Another measure one can construct to observe this dephasing is the time-dependent overlap $\bigcirc$(GR, CS), defined as

$$\bigcirc(A, B) := h_+^A h_+^B + h_\times^A h_\times^B, \tag{60}$$

which we can normalize by using the quantity

$$\bigcirc_N(\mathrm{GR}, \mathrm{CS}) := \sqrt{\bigcirc(\mathrm{GR}, \mathrm{GR}) \bigcirc(\mathrm{CS}, \mathrm{CS})}. \tag{61}$$

This measure is related to the integrand of the overlap commonly used in gravitational-wave data analysis. Figure 6 plots $\bigcirc(\mathrm{GR}, \mathrm{CS})/\bigcirc_N$ as a function of time. Observe that after only three weeks of data (roughly $10^5 M$ of evolution), systems (A) and (B) will probably not be able to distinguish between GR and CS geodesics.

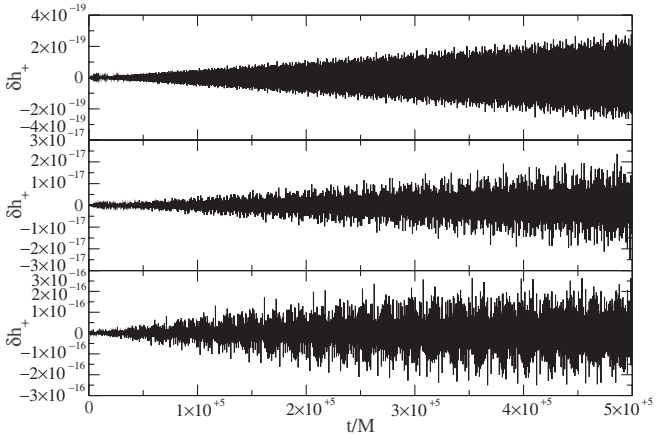

FIG. 5. Dephasing of the GW polarization h_+ as a function of time. The top panel corresponds to system (A), the middle one to system (B) and the bottom one to system (C).

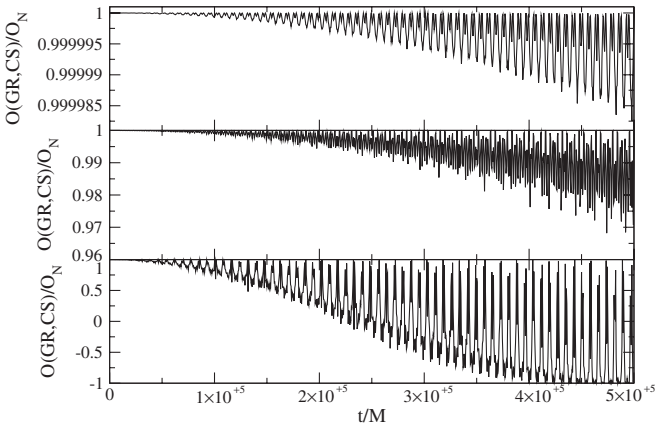

FIG. 6. Running average of the normalized dephasing measure $\bigcirc$(GR, CS) over 20 consecutive time steps as a function of time. The top panel corresponds to system (A), the middle one to system (B) and the bottom one to system (C).

On the other hand, system (C) will probably be able to distinguish this difference, because it experiences a deeper gravitational potential. This plot shows how robust LISA gravitational-wave astronomy can be when considering geodesic motion about a spinning MBH, since even a rather strong curvature correction to the action leads to gravitational waves that are virtually indistinguishable from GR ones, unless the SCO is close to the light ring or the coupling constant of the curvature correction is quite large.

By considering system (C), the most relativistic one, one can ask how small can ζ or, more precisely, ξ be in order to cause a loss in the normalized dephasing measure of about 5% after $10^5 M$ of evolution [Eqs. (60) and (61)]. The answer can be found in Fig. 7, which shows the average of the normalized dephasing measure as a function of time

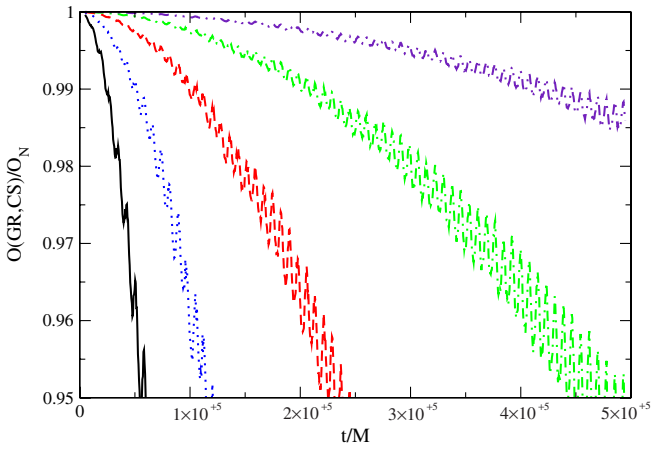

FIG. 7 (color online). Normalized dephasing measure $\mathcal{O}$(GR, CS) as a function of time for system (C) using: $\xi = 0.4M^4$ (solid black), $\xi = 0.2M^4$ (dotted blue), $\xi = 0.1M^4$ (dashed red), $\xi = 0.05M^4$ (dotted-dashed green), and $\xi = 0.025M^4$ (dotted-dotted-dashed violet).

for system (C), but for the following values of the CS parameter: $\xi = 0.4M^4$ (solid black), $\xi = 0.2M^4$ (dotted blue), $\xi = 0.1M^4$ (dashed red), $\xi = 0.05M^4$ (dotted-dashed green), and $\xi = 0.025M^4$ (dotted-dotted-dashed violet). Observe that over 4 months of data, the CS correction could lead to a significant dephasing even for a CS parameter of $\mathcal{O}(10^{-2})$. On the other hand, if one integrates incoherently over three-week segments of the data, then the CS correction would lead to a dephasing only if the CS parameter is of $\mathcal{O}(10^{-1})$. In this case, however, one would have trouble connecting three-week segments together if the CS correction is not taken into account.

Another important question is how this bound compares with bounds obtained from binary pulsar tests. The precession of the perigee in binary pulsars can be used to argue that $\xi^{1/4} \lesssim 10^4$ km, as was done in paper I. For inspirals, a GW test of DCSMG can be expressed as

$$\xi^{1/4} \lesssim 6 \times 10^6 \delta^{1/4} (M/M_\bullet) \text{ km}, \tag{62}$$

where δ here represents the accuracy to which we can measure ξ. This accuracy depends not only on the integration time, the signal-to-noise ratio and the type of orbit considered, but it should also be enhanced if one accounts for radiation-reaction effects, since they are also CS corrected (see Sec. VI). Based on the results of this section, it is not ludicrous to expect that $\delta \sim 10^{-6}$ or better depending on the system, while one also sees that IMRIs are favored over EMRIs due to the M^{-1} dependence. Thus, if one considers an IMRI with total mass $M = 10^3 M_\odot$, and if one assumes $\delta = 10^{-6}$, then the constraint can be better than the binary pulsar one by at least 2 orders of magnitude. Moreover, as we shall see in Sec. VI, radiation-reaction effects depend on the oscillatory sector of the CS scalar, which in turn affects GWs directly. Such an oscillatory sector of the theory is simply *untestable* by binary pulsar experiments.

The results and arguments presented above suggest that GW observations with LISA could allow for interesting tests of DCSMG, but of course, these arguments should be backed up by a deeper and more thorough data analysis study. In this sense, the figures presented in this section should only be taken as an indication of the possible dephasing and loss of overlap that one could experience if CS theory is in play. A detailed study of the dependence of such a test on the spectral noise density curve, the location of the detector in the sky via the beam pattern functions, and the distance to the source is thus of key importance, but postponed to future work.

VI. GRAVITATIONAL-WAVE PROPAGATION AND RADIATION REACTION

The semirelativistic approximation provides a sensible approximation to the emission of GWs generated by the motion of SCOs around MBHs, but so far radiation reaction has been completely neglected. These effects can be incorporated via the adiabatic approximation [47,48,50–52], that is, the assumption that the changes in the *constants* of motion (E, L, Q) evolve in a time scale much larger than the orbital ones. In this scheme, one then argues that the system can be evolved using a geodesic evolution for a certain number of orbital cycles, after which the constants of motion are corrected by estimates that use balance laws (e.g. the GR energy balance law provides a prescription of how to modify the orbital energy due to GW energy emission out to infinity and into the horizon).

In order to obtain the balance laws one must understand the propagation of GWs in the underlaying theory and their associated, effective stress-energy tensor. This can be done in the framework of the shortwave approximation, where one decomposes the geometry into a background and an oscillatory part corresponding to GWs. Such a decomposition holds when the GW wavelength is much smaller than the typical length scale associated with the background curvature.

In this section, we develop the shortwave approximation for DCSMG and compute the effective stress-energy tensor of GWs in this theory. Based on this, and using the symmetries of the background geometry (timelike and axial Killing vectors), we can establish balance laws that can allow us to introduce radiation-reaction effects, in the adiabatic approximation, in the energy and angular momentum. For the case of the Carter constant the situation is more difficult as it is not associated with a Killing vector symmetry, but perhaps a two-time-scale expansion could be performed, similar to that introduced in [97].

A. The short-wavelength approximation

The short-wavelength approximation (SWA) was first introduced by Isaacson [98,99] (see also [63] and references therein) to study the propagation of GWs beyond the linear approximation. In the SWA one assumes that the typical GW wavelength $\lambda_{\rm GW}$ is much smaller than the curvature length scale $\mathcal{R}$ such that $\lambda_{\rm GW} \ll \mathcal{R}$, where $\mathcal{R}^{-2}$ is the typical scale of the components of the Riemann tensor. In this way, we can split the spacetime metric into a background metric $\bar{\mathrm{g}}_{\mu\nu}$, with associated curvature scale $\mathcal{R}$, plus an *oscillating* metric perturbation describing the GWs $h_{\mu\nu}$, with an associated length scale $\lambda_{\rm GW}$ [see e.g. Eq. (8)] and an associated amplitude $h_{\rm GW}$. In this way, $\partial_\alpha \bar{\mathrm{g}}_{\mu\nu} \sim 1/\mathcal{R}$ and $\partial_\alpha h_{\mu\nu} \sim h_{\rm GW}/\lambda_{\rm GW}$.

In practice, applying the SWA to any tensor implies separating its background part from its oscillatory part, which can be done by averaging over several wavelengths ($\lambda_{\rm GW}$). Such separation can be accomplished via the Brill-Hartle averaging procedure [98,99], which applies to convex regions of the background spacetime (regions where any two points can be joined by a unique geodesic). Then, the average of the components of a given tensor $T^{a_1\cdots}{}_{b_1\cdots}$ is defined as

$$\langle T^{a_1\cdots}_{b_1\cdots}\rangle(x) := \int_{\mathcal{W}} d^4x' \sqrt{-\bar{g}(x')} f(x', x) \hat{g}^{a_1}_{a'_1}(x, x') \ldots \times \hat{g}^{b'_1}_{b_1}(x, x') \ldots T^{a'_1\cdots}_{b'_1\cdots}(x'), \quad (63)$$

where the integration takes place over a *small* region $\mathcal{W}$ containing several GW wavelengths; $\hat{g}^{a_1}{}_{a'_1}$ is the bitensor of parallel displacement in the background spacetime; and $f(x', x)$ is a weighting function that smoothly decays to zero as x and x' are separated by many wavelengths. The main properties of this averaging rule (for details see [63]) are as follows:

(i) Background covariant derivatives commute [fractional errors are of $\mathcal{O}(\lambda_{\rm GW}/\mathcal{R})^2$].
(ii) Total divergences average out to zero [fractional errors are of $\mathcal{O}(\lambda_{\rm GW}/\mathcal{R})$].
(iii) As a corollary of (i) and (ii), one can freely integrate by parts.

These rules shall be used heavily in the next section to obtain an expressions for the GW stress-energy tensor in CS modified gravity.

B. Effective stress-energy tensor for GWs

In DCSMG, not only does the metric tensor oscillate, but also the CS scalar field, sourced exclusively by the spacetime curvature [see Eq. (5)]. When GWs are present, these will then generically induce oscillations in the CS scalar field, which forces us to also decompose ϑ into a background part $\bar{\vartheta}$ and an oscillatory part $\tilde{\vartheta}$, the latter induced by GWs.

Let us now study the field equations in the SWA, which requires expansions up to second order in the oscillatory parts (see Appendix B 1 for the basic formulas used for these expansions). The structure of the resulting equations consists of oscillatory terms, linear in the amplitude, and *coarse-grained* terms that describe how the background is modified by GWs. This modification is produced by the *averaged* second-order term in the oscillatory part, which reflects the nonlinear character of this effect.

Then we set to zero the linear part in the wave amplitude, $h_{\rm GW}$, obtaining in this way the equations that describe the propagation of the waves in the background. In GR, these equations are simply

$$^{(1)}R_{\mu\nu} = -\frac{1}{2}h_{\mu\nu|\rho}{}^{\rho} + \mathcal{O}\left(\frac{h_{\rm GW}}{\mathcal{R}^2}\right) = \frac{1}{2\kappa}\left({}^{(1)}T^{\rm mat}_{\mu\nu} - \frac{1}{2}h_{\mu\nu}T^{\rm mat} - \frac{1}{2}\bar{g}_{\mu\nu}{}^{(1)}T^{\rm mat}\right), \quad (64)$$

where we have used the Lorenz gauge [Eq. (9)] and where, here and in the rest of this section, the superscript preceding a given quantity denotes the perturbative order of this quantity with respect to metric perturbations (see Appendix B for more details).

In DCSMG the propagation equations have the following form:

$$^{(1)}R_{\mu\nu} + \frac{\alpha}{\kappa}({}^{(1)}C_{\mu\nu}[\bar{\vartheta}, h] + C_{\mu\nu}[\tilde{\vartheta}, \bar{g}]) = \frac{1}{2\kappa}\Big[{}^{(1)}T^{\rm mat}_{\mu\nu} + {}^{(1)}T^{(\vartheta)}_{\mu\nu}[\bar{\vartheta}] + \delta T^{(\vartheta)}_{\mu\nu}[\bar{\vartheta}, \tilde{\vartheta}] - \frac{1}{2}h_{\mu\nu}(T^{\rm mat} + T^{(\vartheta)}[\bar{\vartheta}]) - \frac{1}{2}\bar{g}_{\mu\nu}({}^{(1)}T^{\rm mat} + {}^{(1)}T^{(\vartheta)}[\bar{\vartheta}] + \delta T^{(\vartheta)}[\bar{\vartheta}, \tilde{\vartheta}])\Big], \quad (65)$$

$$\beta\{\bar{\Box}\,\tilde{\vartheta} - \bar{g}^{\alpha\beta(1)}S^{\lambda}_{\alpha\beta}\bar{\vartheta}_{|\lambda} - h^{\alpha\beta}\bar{\vartheta}_{|\alpha\beta}\} = -\frac{\alpha}{2}\left\{{}^{*}\bar{R}^{(1)}R[h] + \frac{1}{4}h^{*}\bar{R}\bar{R}\right\}. \quad (66)$$

The detailed structure of Eq. (65) as well the form of $\delta T^{(\vartheta)}_{\mu\nu}[\bar{\vartheta}, \tilde{\vartheta}]$ can be found in Appendix B 2 [Eq. (B31)]. The object ${}^{(1)}S^{\mu}_{\alpha\beta}$ in Eq. (66) denotes the perturbation of the Christoffel symbols and its expression is given in Eq. (B9).

Using the averaging procedure described above, the field equations tell us how the nonlinear contribution of the waves shapes the background. This contribution can be written as an effective stress-energy tensor of the GWs $T^{\rm GW}_{\mu\nu}$ (the Isaacson tensor), allowing us to write

$$\bar{G}_{\mu\nu} + \frac{\alpha}{\kappa}\bar{C}_{\mu\nu} = \frac{1}{2\kappa}(T^{\rm mat}_{\mu\nu} + T^{(\vartheta)}_{\mu\nu}[\bar{\vartheta}] + T^{(\vartheta)}_{\mu\nu}[\tilde{\vartheta}] + T^{\rm GW}_{\mu\nu}). \quad (67)$$

In GR, the Isaacson tensor is given by (see e.g. [63])

$$T^{\rm GW}_{\mu\nu} = -2\kappa\{\langle{}^{(2)}R_{\mu\nu}[h]\rangle - \tfrac{1}{2}\bar{g}_{\mu\nu}\langle{}^{(2)}R[h]\rangle\}, \quad (68)$$

which, using the expressions in Appendix B and working in the Lorenz gauge [Eq. (9)] supplemented with the traceless condition [Eq. (10)], reduces to

$$T^{\rm GW}_{\mu\nu} = \frac{\kappa}{2}\langle h_{\alpha\beta|\mu}h^{\alpha\beta}{}_{|\nu}\rangle. \quad (69)$$

One can see, using the first-order equations and the average rule, that this tensor is traceless and divergence-free within the errors produced by the approximations made using the SWA scheme:

$$\bar{g}^{\mu\nu}T^{\rm GW}_{\mu\nu} = 0, \qquad T^{{\rm GW}|\nu}_{\mu\nu} = 0. \quad (70)$$

In DCSMG, the effective stress-energy tensor of GWs is given by

$$T^{\rm GW}_{\mu\nu} = -2\kappa\Big\{\langle{}^{(2)}R_{\mu\nu}[h]\rangle - \frac{1}{2}\bar{g}_{\mu\nu}\langle{}^{(2)}R[h]\rangle + \frac{\alpha}{\kappa} \times (\langle{}^{(2)}C_{\mu\nu}[\bar{\vartheta}, h]\rangle + \langle{}^{(1)}C_{\mu\nu}[\tilde{\vartheta}, h]\rangle)\Big\}. \quad (71)$$

Again, using the formulas in Appendix B, restricted to the TT gauge of Eqs. (9) and (10), and the properties of the

averaging (in particular, the integration by parts), we find that the terms corresponding to the CS correction *vanish exactly*, yielding the same expression as in GR (for a guided explanation of this fact, see Appendix B). That is, the effective stress-energy tensor of GWs in DCSMG [which enters in Eq. (67)] is simply given by Eq. (68) or (69), which implies that the backreaction in the orbital motion due to GW emission is essentially as in GR.

We can now look at the equation for ϑ with the second-order corrections. This is a linear equation in ϑ and hence all the modifications come from second-order terms in the GW. One the finds that

$$\beta\bar{\Box}\,\bar{\vartheta} = -\frac{\alpha}{4}\left(1-\frac{1}{4}\langle h^{\alpha\beta}h_{\alpha\beta}\rangle\right)^{*}\bar{R}\bar{R} - \frac{\alpha}{4}\bar{\epsilon}_{\alpha\beta\mu\nu}\langle {}^{(1)}R^{\alpha\beta\rho\sigma(1)}R_{\rho\sigma}{}^{\mu\nu}\rangle. \quad (72)$$

As we can see there are two second-order corrections to the background value of the CS scalar field: one that *renormalizes* the value of α, $\langle h^{\alpha\beta}h_{\alpha\beta}\rangle \sim h^2_{\rm GW}$, and another that scales as $\alpha h^2_{\rm GW}/\lambda^4_{\rm GW}$.

C. Balance laws and radiation-reaction effects

By means of the SWA we have studied the propagation of GWs and of oscillations induced in the CS scalar field. We have also seen how these oscillations affect the background values of the metric tensor [Eq. (67)] and of the CS scalar field [Eq. (72)]. Of particular importance is the equation for the modification of the background geometry, which contains the effective stress-energy tensor of the GWs, which we have found has the same form as in GR. From the previous development it is clear that from Eq. (67) we have the following conservation equation:

$$\bar{\nabla}^{\nu}\tau_{\mu\nu} = 0, \qquad \tau_{\mu\nu} = T^{\rm mat}_{\mu\nu} + T^{(\vartheta)}_{\mu\nu}[\tilde{\vartheta}] + T^{\rm GW}_{\mu\nu}, \quad (73)$$

where we have used that the background Einstein tensor is divergence-free and the equations of motion for the background scalar field $\bar{\vartheta}$ are satisfied. The new ingredient with respect to GR is the appearance of the stress-energy tensor associated with the oscillations induced in the CS scalar field.

Here, the background clearly corresponds to the MBH geometry and the CS background scalar field is given in Eqs. (19) and (20). Using the Killing symmetries of the background, described by the vector fields t^{μ} and ψ^{μ} [see Sec. III B], the vector fields

$$\mathcal{E}^{\mu} = -\tau^{\mu}{}_{\nu}t^{\nu}, \qquad \mathcal{J}^{\mu} = \tau^{\mu}{}_{\nu}\psi^{\nu}, \quad (74)$$

describe the total fluxes of energy and angular momentum and are, by virtue of Eq. (73) and the Killing equations, divergence-free vector fields. Therefore, we can obtain balance laws for the energy and angular momentum by considering a spacetime region $\mathcal{V}$ with boundary $\partial\mathcal{V}$ and integrating over it the divergence-free conditions: $\mathcal{E}^{\mu}{}_{|\mu} = 0$ and $\mathcal{J}^{\mu}{}_{|\mu} = 0$.

For the study of IMRI/EMRIs one can take $\mathcal{V} = \{(t, r, \theta, \phi),$ such that $t_o < t < t_f$ and $r_H < r < r_I\}$, where the inner radius r_H can be taken to be close to the horizon location and the outer radius r_I can be taken to be effectively close to infinity (or at least far away from the SCO). In this way $\partial\mathcal{V}$ is composed of two *cylinders* (one at $r = r_H$ and the other one at $r = r_I$) of finite size, limited by two slices, one at an initial time $t = t_o$ and the other one at a final time $t = t_f$.

The balance laws for energy and angular momentum tell us that the change in the constants of motion (E, L) is given by the amount of energy/angular momentum, of the GWs and of the CS scalar field, flowing away from $\mathcal{V}$ to infinity $(r = r_I)$ and into the MBH horizon $(r = r_H)$. In this way, one can account for the radiation-reaction effects in the adiabatic approximation. Note that this only takes care of the changes in the energy and in the angular momentum of the SCO, while the question of how to correct the third constant of motion, the Carter constant Q, in a general way remains still open (see [48–52] for recent advances on that question).

The flux of energy (or energy luminosity) in GWs going towards infinity is given by

$$\frac{dE_{\rm GW}}{dt} = -\lim_{r\to\infty} r^2 \int_{S^2_\infty} d\Omega\, T^{\rm GW}_{ti} n^i, \quad (75)$$

where $n^i = x^i/r$ is the unit normal to the surfaces $r =$ const near spatial infinity, where the background geometry is essentially flat. Although the expression for the energy luminosity [Eq. (75)] is formally the same as in GR, the luminosities are actually different because the geodesic equations are indeed CS corrected by the modified Kerr background given in Eq. (19).

To illustrate this difference, let us consider the expression

$$\frac{dE_{\rm GW}}{dt} = \kappa(\dot{h}^2_{+} + \dot{h}^2_{\times}), \quad (76)$$

where h_{+} and $h_{\times}$ are the GW plus and cross polarizations, respectively, which one can obtain from Eqs. (69) and (75). Figure 8 plots the difference between the energy flux computed from the GW emission of a SCO moving in geodesics of Kerr and a SCO moving in geodesics of the CS modified Kerr metric [Eq. (19)], for systems (A) (top panel), (B) (middle panel) and (C) (bottom panel) as a function of time. For reference, the maximum magnitude of the energy flux computed from geodesic waveforms about Kerr are $3\times10^{-37}M^{-2}$ for system (A), $3\times10^{-36}M^{-2}$ for system (B) and $2\times10^{-35}M^{-2}$ for system (C). Observe that, after approximately four months of evolution, the fractional correction to the luminosities by the CS correction is about 1% for system (A), 10% for system (B) and about 50% for system (C). As expected, the

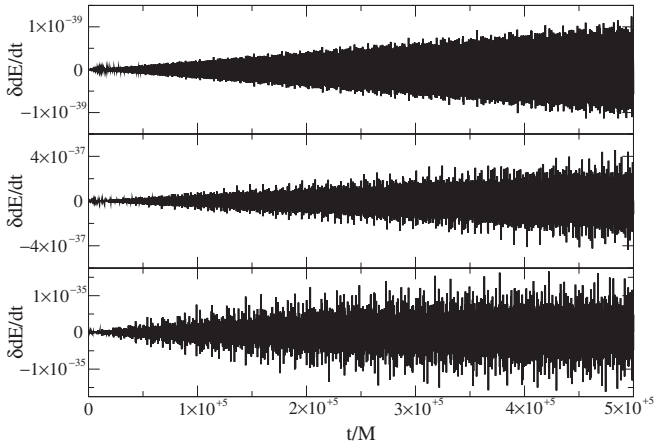

FIG. 8. Energy flux difference (in units of M^{-2}) between the flux computed with gravitational waves produced by geodesics about Kerr and about the CS modified Kerr background for systems (A) (top panel), (B) (middle panel) and (C) (bottom panel) as a function of time.

more relativistic the system, the larger the CS correction to the waveforms, and therefore, the larger the effect on radiation reaction. Such corrections could have a significant impact on kludge-type waveforms, when one takes into account that the GW energy lost must also be supplemented by the energy emitted by the CS scalar field [see the conservation equation, Eq. (73)]. To include this contribution, one would need to solve the evolution equation for the CS scalar field [Eq. (46)], using as input the gravitational waveform computed without radiation reaction.

The machinery developed in this paper allows, for the first time, the inclusion of these radiation-reaction effects in the orbital evolution of EMRIs and IMRIs in a realistic, alternative theory of gravity. With these developments, one can now properly construct alternative-theory, kludge waveforms.

VII. CONCLUSIONS

We have studied the effects of dynamical CS modified gravity on the orbit and GWs generated by IMRIs and EMRIs. The semirelativistic approximation was employed, through which we modeled the SCO trajectory via the geodesic equations, while we treated GWs through a multipolar generation formalism.

We began by showing that test particles follow geodesics in DCSMG. We then proceeded to explicitly calculate the modified geodesic equations for a test particle in a generic orbit around a CS modified Kerr MBH [25]. We showed that the fundamental frequencies of the modified background are CS modified, as well as the relations between the MBH multipole moments and its mass and spin, although the latter incurs corrections at $\ell = 4$ multipolar order, which might be small to be detected by future GW observations with LISA.

We then continued with the study of GW generation in the modified theory. We saw that the GW generation formula based on the multipolar expansion is corrected to leading order by second-order terms of $\mathcal{O}(\mu\zeta)$, which we neglect here. This GW generation formalism is also modified by GR radiation-reaction effects, which scale as the square of the mass ratio and which we also neglect here.

We then evolved geodesics in this modified background and compared their associated GWs to those generated by geodesics on a pure Kerr background. Generically, we find that these waves dephase after a certain number of cycles that depends on the strength of the CS coupling parameter, as well as on how relativistic the geodesic under consideration is and the signal-to-noise ratio of the event. For small CS parameters, such a dephasing is small, leading to mismatches that will not affect GW detection. These mismatches, however, might affect GW characterization, leading to erroneous conclusions about the orbital parameters of the system.

EMRIs and IMRIs can thus be used to probe DCSMG, both by constraining the CS coupling strength to unprecedented levels, as well as to sample the oscillatory dynamic sector of the CS scalar field. Moreover, the study presented can be viewed as an explicit example of the effect a non-Kerr background could have on GWs, where in this case the non-Kerrness arises from a well-defined and physically well-motivated alternative theory. Since this modified theory introduces a higher-order curvature correction, modifications to the Kerr metric are only dominant in the strong field and cannot be sampled by the waveform's first multipoles.

The analysis presented here employs some approximations that lead to certain inaccuracies, which we list here: (i) neglecting radiation reaction in the dynamics, which scales with the square of the mass ratio; (ii) neglecting the curvature of the background for the propagation of the gravitational waves from the source to infinity; (iii) neglecting CS modifications to the GW emission, which scale with the product of the mass ratio and the CS coupling constants; (iv) neglecting CS modifications to the MBH background metric that are of third order in the spin parameter and the small-coupling approximation. Whether one effect is dominant over the others depends on the strength of the CS coupling constants, which is at present unknown and essentially unconstrained. In particular, except for the obvious scaling with the mass ratio, it is difficult to estimate the magnitude of effect (ii), which is one of the main ingredients of the semirelativistic approximations. Comparisons made in [58], however, indicate that inaccuracies arising from the semirelativistic approximation are acceptable for certain data analysis purposes, suggesting that perhaps inaccuracies associated with effects (i) and (iv) are dominant here. We do not expect these inaccuracies to affect the main conclusions derived in this paper, i.e. that DCSMG leads to a strong-field modi-

fication to GW generation that could be used to constrain the theory with future LISA observations of EMRIs.

Future work could concentrate on the inclusion of radiation reaction in an adiabatic fashion to the waveforms presented here. Such a task in the modified theory is rather straightforward since these dissipative effects are CS corrected only through the emission of a CS scalar field. One could then supplement the standard GR expressions for the rate of change of the geodesic constants of motion by these CS corrections to allow for a true, kludgelike, inspiral. Although the CS correction does not modify radiation reaction through changes in the Isaacson tensor, dissipative effects will accentuate the observed dephasing.

Once such radiation-reaction effects are included, a thorough data analysis study should be carried out to confirm or not the expectations presented in this paper. Of particular importance will be the inclusion of the beam pattern functions and the motion of the detector in the sky, which have been shown to be relevant for parameter estimation [100–103]. Moreover, the computation of the proper overlap and Fisher matrix would include the spectral noise density curve of the detector, as well as details of the sensitivity of the modified waveforms on the parameters of the alternative theory.

Another avenue for future research is the inclusion of the leading-order CS correction to the GW emission framework. We have provided here a map, albeit involved, to construct such a correction which is based on black hole perturbation theory. Another possibility would be to study GW generation in the context of a post-Newtonian/post-Minkowskian expansion and asymptotic matching [104–108]. Although this formalism is formally valid in the slow-motion approximation, so is the truncated multipolar decomposition used here.

Last but not least, an exact metric that describes spinning MBHs with arbitrary spin angular momentum in DCSMG is still lacking. The results presented here are in principle valid only in the slow-rotation approximation. Generalizing such results to higher order in a perturbative fashion could be dramatically difficult, since to next order the scalar stress-energy tensor will also contribute to the modified field equations. Perhaps, a full numerical study of the collapse of a scalar field with angular momentum would be appropriate to disentangle the effects of DCSMG on rapidly rotating MBH backgrounds.

ACKNOWLEDGMENTS

We would like to thank Bernard Schutz for encouraging us to study EMRIs in the context of CS modified gravity. We would also like to thank Stephon Alexander, Emanuele Berti, Vitor Cardoso, Daniel Grumiller, Scott Hughes, Ben Owen, Frans Pretorius, David Spergel, Paul Steinhardt and Shaun Wood, for helpful discussions. C. F. S. acknowledges support from the Ramón y Cajal Programme of the Ministry of Education and Science of Spain, by a Marie Curie International Reintegration Grant (No. MIRG-CT-2007-205005/PHY) within the 7th European Community Framework Program, and from Contract No. ESP2007-61712 of the Spanish Ministry of Education and Science. He also acknowledges the hospitality of the Physics Department at Princeton University during a visit where this work was completed, and the CSIC for financial support for this visit. N. Y. acknowledges support from NSF Grant No. PHY-0745779 and also acknowledges the hospitality of the Institut de Ciències de l'Espai (CSIC-IEEC) during the realization of this work.

APPENDIX A: PLANE WAVES IN DCSMG

Here we present a brief study of the main properties of a class of exact solutions describing plane-fronted gravitational waves (*pp waves*) in DCSMG (see [24] for pp waves in the nondynamical formalism). This study illustrate the results found in Sec. II C regarding the polarization properties of GWs in DCSMG. The line element for pp waves can be written as (see e.g. [109])

$$ds^2 = -2dudv - H(u,x,y)du^2 + dx^2 + dy^2, \tag{A1}$$

where $u = t - z$ and $v = t + z$ are retarded and advance null coordinates, respectively (the waves propagate along the z axis), the wave fronts are given by the null planes $u =$ const, and all physical information is encoded in the scalar H. Indeed, using a Newman-Penrose null basis [109,110] adapted to pp waves [$\boldsymbol{k} = \partial_v$, $\ell = \partial_u - (H/2)\partial_v$, $\boldsymbol{m} = (\partial_x + i\partial_y)/\sqrt{2}$] one finds that the only two nonvanishing Newman-Penrose complex curvature scalars are

$$\Psi_4 = \tfrac{1}{4}(\partial_x^2 - \partial_y^2 + 2i\partial_{xy}^2)H, \qquad \Phi_{22} = \tfrac{1}{4}(\partial_x^2 + \partial_y^2)H. \tag{A2}$$

Considering an arbitrary CS scalar field, $\vartheta = \vartheta(u,v,x,y)$ and the metric in Eq. (A1), the modified field equations [Eqs. (4) and (5)] force us to

$$\vartheta = \vartheta(u), \qquad (\partial_x^2 + \partial_y^2)H = \frac{\beta}{\kappa}\dot{\vartheta}^2, \tag{A3}$$

where $\vartheta(u)$ is an arbitrary function and $\dot{\vartheta} = d\vartheta/du$. From Eqs. (A2) and (A3) we see that in GR ($\beta = 0$) the only nonvanishing Weyl complex scalar is Ψ_4, which encodes the two GR GW polarizations. In DCSMG, there is an extra degree of freedom due to the real Ricci scalar Φ_{22}, which describes a transverse GW whose effect on a ring of test particles is to either expand or contract it maintaining a circular shape (a so-called *breathing* mode) [67]. The nonvanishing of Ψ_4 and Φ_{22} suggests naively that DCSMG is of type N_3 (like the Dicke-Brans-Jordan theory [111]), but on closer inspection Φ_{22} is of $\mathcal{O}(\dot{\theta}^2)$, and thus the theory reduces to type N_2 (the same as GR) in the weak-amplitude approximation that is required in the $E(2)$ classification.

This new polarization state can be studied more cleanly by considering *plane* waves [112], a special class of pp

waves characterized by a scalar H that is quadratic in x and y (Ψ_4 and Φ_{22} are independent of x and y and the metric has a five-dimensional Lie group of Killing symmetries [109]). Terms linear in x and y can be removed by coordinate transformations that leave invariant the line element in Eq. (A1). The solution to Eq. (A3) can then be written as

$$H(u, x, y) = A(u)(x^2 - y^2) + 2B(u)xy + C(u)(x^2 + y^2), \tag{A4}$$

where $A(u)$ and $B(u)$ are arbitrary functions and $C(u) = (\beta/(4\kappa))\dot{\vartheta}^2$. From (A2) one finds that $\Psi_4 = A + iB$ and $\Phi_{22} = C$, clearly showing that the extra non-GR polarization corresponds to a breathing mode. In the weak-amplitude regime, however, $\vartheta^2 \simeq 0$, and the effect of this extra polarization is negligible, thus establishing the result that DCSMG only dominantly excites the same two GW polarization states excited in GR.

APPENDIX B: FORMULAS FOR THE SHORT-WAVELENGTH APPROXIMATION

In this appendix we provide some of the formulas that we have computed and used to derive the form of the effective stress-energy tensor of GWs for DCSMG, using the SWA. However, these are generic perturbative expansions (induced only by perturbations of the metric tensors) of geometric quantities which can be used in other perturbative schemes, although the interpretation of the different terms would be different.

1. Second-order expansion

Given the splitting of the spacetime metric given in Eq. (8), we need to perform an expansion in $h_{\mu\nu}$ to second order of the different geometric quantities involved in the CS modified gravitational field equations. The inverse of the metric is

$$\mathrm{g}^{\mu\nu} = \bar{\mathrm{g}}^{\mu\nu} - h^{\mu\nu} + h^{\mu}{}_{\rho}h^{\rho\nu} + \mathcal{O}(h^3), \tag{B1}$$

where

$$\begin{aligned} h^{\mu}{}_{\nu} = \bar{\mathrm{g}}^{\mu\rho}h_{\rho\nu}, \qquad h_{\mu}{}^{\nu} = \bar{\mathrm{g}}^{\nu\rho}h_{\mu\rho}, \\ h^{\mu\nu} = \bar{\mathrm{g}}^{\mu\rho}\bar{\mathrm{g}}^{\nu\sigma}h_{\rho\sigma}. \end{aligned} \tag{B2}$$

The expansion of the metric determinant $\mathrm{g} = \det(\mathrm{g}_{\mu\nu})$ is then given by

$$\mathrm{g} = \bar{\mathrm{g}}\{1 + h + \tfrac{1}{2}(h^2 - h^{\mu\nu}h_{\mu\nu}) + \mathcal{O}(h^3)\}. \tag{B3}$$

From here we can expand the completely antisymmetric Levi-Civita volume four-form:

$$\epsilon_{\mu\nu\rho\sigma} = \sqrt{-\mathrm{g}}\,\delta^{0123}_{\mu\nu\rho\sigma}, \tag{B4}$$

to get

$$\epsilon_{\mu\nu\rho\sigma} = \bar{\epsilon}_{\mu\nu\rho\sigma}\{1 + \tfrac{1}{2}h + \tfrac{1}{8}(h^2 - 2h^{\alpha\beta}h_{\alpha\beta}) + \mathcal{O}(h^3)\}. \tag{B5}$$

The Christoffel symbols can be written exactly as follows:

$$\Gamma^{\mu}_{\rho\sigma} = \bar{\Gamma}^{\mu}_{\rho\sigma} + S^{\mu}_{\rho\sigma}, \tag{B6}$$

where $S^{\mu}_{\rho\sigma}$ is

$$S^{\mu}_{\rho\sigma} = \tfrac{1}{2}\mathrm{g}^{\mu\nu}(h_{\sigma\nu|\rho} + h_{\rho\nu|\sigma} - h_{\rho\sigma|\nu}). \tag{B7}$$

This tensor can be expanded in $h_{\mu\nu}$ yielding

$$S^{\mu}_{\rho\sigma} = {}^{(1)}S^{\mu}_{\rho\sigma} + {}^{(2)}S^{\mu}_{\rho\sigma} + \mathcal{O}(h^3), \tag{B8}$$

where

$${}^{(1)}S^{\mu}_{\rho\sigma} = \tfrac{1}{2}\bar{\mathrm{g}}^{\mu\nu}(h_{\sigma\nu|\rho} + h_{\rho\nu|\sigma} - h_{\rho\sigma|\nu}), \tag{B9}$$

$${}^{(2)}S^{\mu}_{\rho\sigma} = -\tfrac{1}{2}h^{\mu\nu}(h_{\sigma\nu|\rho} + h_{\rho\nu|\sigma} - h_{\rho\sigma|\nu}). \tag{B10}$$

The introduction of the tensor $S^{\mu}_{\rho\sigma}$ is convenient since it can be used to simplify the expressions for the expansions of the Riemann tensor and derived geometric quantities. An exact expression relating the Riemann tensor of the spacetime to the background one through the tensor $S^{\mu}_{\rho\sigma}$ is

$$R^{\alpha}{}_{\beta\mu\nu} = \bar{R}^{\alpha}{}_{\beta\mu\nu} - 2S^{\alpha}_{\beta[\mu|\nu]} + 2S^{\alpha}_{\rho[\mu}S^{\rho}_{\nu]\beta}. \tag{B11}$$

Therefore, an exact expression for the Ricci tensor is

$$R_{\beta\nu} = \bar{R}_{\beta\nu} + S^{\alpha}_{\beta\nu|\alpha} - S^{\alpha}_{\alpha\beta|\nu} + S^{\alpha}_{\alpha\rho}S^{\rho}_{\beta\nu} - S^{\alpha}_{\rho\nu}S^{\rho}_{\beta\alpha}. \tag{B12}$$

From these expressions of the Riemann and Ricci tensors we can immediately write down their first- and second-order terms in the perturbative expansion in $h_{\mu\nu}$. For the Riemann tensor they are

$${}^{(1)}R^{\alpha}{}_{\beta\mu\nu} = -2{}^{(1)}S^{\alpha}_{\beta[\mu|\nu]}, \tag{B13}$$

$${}^{(2)}R^{\alpha}{}_{\beta\mu\nu} = -2{}^{(2)}S^{\alpha}_{\beta[\mu|\nu]} + 2{}^{(1)}S^{\alpha}_{\rho[\mu}{}^{(1)}S^{\rho}_{\nu]\beta}, \tag{B14}$$

and for the Ricci tensor

$${}^{(1)}R_{\beta\nu} = {}^{(1)}S^{\alpha}_{\beta\nu|\alpha} - {}^{(1)}S^{\alpha}_{\alpha\beta|\nu}, \tag{B15}$$

$$\begin{aligned} {}^{(2)}R_{\beta\nu} = {}^{(2)}S^{\alpha}_{\beta\nu|\alpha} - {}^{(2)}S^{\alpha}_{\alpha\beta|\nu} + {}^{(1)}S^{\alpha}_{\alpha\rho}{}^{(1)}S^{\rho}_{\beta\nu} \\ - {}^{(1)}S^{\alpha}_{\rho\nu}{}^{(1)}S^{\rho}_{\beta\alpha}. \end{aligned} \tag{B16}$$

The Einstein and Cotton tensors have more complicated expressions. The first- and second-order expansion of the Einstein tensor are

$${}^{(1)}G_{\mu\nu} = {}^{(1)}R_{\mu\nu} - \tfrac{1}{2}\bar{\mathrm{g}}_{\mu\nu}(\bar{\mathrm{g}}^{\rho\sigma(1)}R_{\rho\sigma} - h^{\rho\sigma}\bar{R}_{\rho\sigma}) - \tfrac{1}{2}h_{\mu\nu}\bar{R}, \tag{B17}$$

$$\begin{aligned} {}^{(2)}G_{\mu\nu} = {}^{(2)}R_{\mu\nu} - \tfrac{1}{2}\bar{\mathrm{g}}_{\mu\nu}(\bar{\mathrm{g}}^{\rho\sigma(2)}R_{\rho\sigma} - h^{\rho\sigma(1)}R_{\rho\sigma} \\ + h^{\rho}{}_{\lambda}h^{\lambda\sigma}\bar{R}_{\rho\sigma}) - \tfrac{1}{2}h_{\mu\nu}(\bar{\mathrm{g}}^{\rho\sigma(1)}R_{\rho\sigma} - h^{\rho\sigma}\bar{R}_{\rho\sigma}). \end{aligned} \tag{B18}$$

The expansion of the first piece of the Cotton tensor $C^{1}_{\mu\nu}$ is

determined by the following expressions [we remark that these are expansions only in the metric tensor; the CS scalar field is assumed here to be fixed]:

$$
\begin{aligned}
{}^{(1)}C^{1}_{\mu\nu} &= \vartheta_{|\sigma}\bar{\epsilon}_{(\mu}{}^{\sigma\alpha\beta}\{{}^{(1)}R_{\nu)\beta|\alpha} - {}^{(1)}S^{\rho}_{\nu)\alpha}\bar{R}_{\beta\rho}\} \\
&\quad + \vartheta_{|\sigma}{}^{(1)}\epsilon_{(\mu}{}^{\sigma\alpha\beta}\bar{R}_{\nu)\beta|\alpha},
\end{aligned}
\tag{B19}
$$

$$
\begin{aligned}
{}^{(2)}C^{1}_{\mu\nu} &= \vartheta_{|\sigma}\bar{\epsilon}_{(\mu}{}^{\sigma\alpha\beta}\{{}^{(2)}R_{\nu)\beta|\alpha} - {}^{(1)}S^{\rho}_{\nu)\alpha}{}^{(1)}R_{\beta\rho} \\
&\quad - {}^{(2)}S^{\rho}_{\nu)\alpha}\bar{R}_{\beta\rho}\} + \vartheta_{|\sigma}{}^{(1)}\epsilon_{(\mu}{}^{\sigma\alpha\beta}\{{}^{(1)}R_{\nu)\beta|\alpha} \\
&\quad - {}^{(1)}S^{\rho}_{\nu)\alpha}\bar{R}_{\beta\rho}\} + \vartheta_{|\sigma}{}^{(2)}\epsilon_{(\mu}{}^{\sigma\alpha\beta}\bar{R}_{\nu)\beta|\alpha},
\end{aligned}
\tag{B20}
$$

where ${}^{(1)}\epsilon^{\sigma}{}_{\mu}{}^{\alpha\beta}$ and ${}^{(2)}\epsilon^{\sigma}{}_{\mu}{}^{\alpha\beta}$ are the first- and second-order expansion terms of $\epsilon^{\sigma}{}_{\mu}{}^{\alpha\beta}$, respectively. In particular, the first-order term is given by

$$
{}^{(1)}\epsilon_{\mu}{}^{\sigma\alpha\beta} = -h^{\sigma}_{\lambda}\bar{\epsilon}_{\mu}{}^{\lambda\alpha\beta} + 2\bar{\epsilon}_{\mu}{}^{\sigma}{}_{\lambda}{}^{[\alpha}h^{\beta]\lambda} + \tfrac{1}{2}h\bar{\epsilon}_{\mu}{}^{\sigma\alpha\beta}.
\tag{B21}
$$

The expansion of the second piece of the Cotton tensor $C^{2}_{\mu\nu}$ is given by

$$
\begin{aligned}
{}^{(1)}C^{2}_{\mu\nu} &= \tfrac{1}{2}\vartheta_{|\sigma\tau}[\bar{\epsilon}_{(\mu}{}^{\sigma\alpha\beta(1)}R^{\tau}{}_{\nu)\alpha\beta} + {}^{(1)}\epsilon_{(\mu}{}^{\sigma\alpha\beta}\bar{R}^{\tau}{}_{\nu)\alpha\beta}] \\
&\quad - \tfrac{1}{2}\vartheta_{|\rho}{}^{(1)}S^{\rho}_{\sigma\tau}\epsilon_{(\mu}{}^{\sigma\alpha\beta}\bar{R}^{\tau}{}_{\nu)\alpha\beta},
\end{aligned}
\tag{B22}
$$

$$
\begin{aligned}
{}^{(2)}C^{2}_{\mu\nu} &= \tfrac{1}{2}\vartheta_{|\sigma\tau}[\bar{\epsilon}_{(\mu}{}^{\sigma\alpha\beta(2)}R^{\tau}{}_{\nu)\alpha\beta} + {}^{(1)}\epsilon_{(\mu}{}^{\sigma\alpha\beta(1)}R^{\tau}{}_{\nu)\alpha\beta} \\
&\quad + {}^{(2)}\epsilon_{(\mu}{}^{\sigma\alpha\beta}\bar{R}^{\tau}{}_{\nu)\alpha\beta}] \\
&\quad - \tfrac{1}{2}\vartheta_{|\rho}{}^{(1)}S^{\rho}_{\sigma\tau}[\bar{\epsilon}_{(\mu}{}^{\sigma\alpha\beta(1)}R^{\tau}{}_{\nu)\alpha\beta} \\
&\quad + {}^{(1)}\epsilon_{(\mu}{}^{\sigma\alpha\beta}\bar{R}^{\tau}{}_{\nu)\alpha\beta}] - \tfrac{1}{2}\vartheta_{|\rho}{}^{(1)}S^{\rho}_{\sigma\tau}\bar{\epsilon}_{(\mu}{}^{\sigma\alpha\beta}\bar{R}^{\tau}{}_{\nu)\alpha\beta}.
\end{aligned}
\tag{B23}
$$

2. Propagation equations in the SWA

The propagation of oscillations in DCSMG using the SWA approximation is described by the first-order equations given in Eq. (65). Here, we analyze the different terms that appear in this equation adopting the TT gauge defined by Eqs. (9) and (10). We also make use of the SWA to simplify the form of some of the terms. Then, taking into account that

$$
{}^{(1)}S^{\alpha}_{\alpha\mu} = 0, \qquad \bar{g}^{\mu\nu}{}^{(1)}S^{\alpha}_{\mu\nu} = 0,
\tag{B24}
$$

the first term in (65) can be written as

$$
{}^{(1)}R_{\mu\nu} = {}^{(1)}S^{\alpha}_{\mu\nu|\alpha} = -\frac{1}{2}h_{\mu\nu|\rho}{}^{\rho} + \mathcal{O}\left(\frac{h_{\rm GW}}{\mathcal{R}^{2}}\right).
\tag{B25}
$$

From Eq. (7) we have

$$
C^{1}_{\mu\nu}[\tilde{\vartheta}, \bar{g}] = \tilde{\vartheta}_{|\sigma}\bar{\epsilon}^{\sigma\alpha\beta}{}_{(\mu}\bar{R}_{\nu)\alpha|\beta} = \mathcal{O}\left(\frac{\tilde{\vartheta}_{\rm GW}}{\lambda_{\rm GW}\mathcal{R}^{3}}\right),
\tag{B26}
$$

$$
C^{2}_{\mu\nu}[\tilde{\vartheta}, \bar{g}] = \tilde{\vartheta}_{|\sigma\delta}{}^{*}\bar{R}^{\delta}{}_{(\mu\nu)}{}^{\sigma} = \mathcal{O}\left(\frac{\tilde{\vartheta}_{\rm GW}}{\lambda^{2}_{\rm GW}\mathcal{R}^{2}}\right),
\tag{B27}
$$

where $\tilde{\vartheta}_{\rm GW}$ denotes the amplitude of the oscillations in the CS scalar field. From Eqs. (B19) and (B22) we can write

$$
{}^{(1)}C^{1}_{\mu\nu}[\bar{\vartheta}, h] = [\bar{\vartheta}_{|\sigma}\bar{\epsilon}_{(\mu}{}^{\sigma\alpha\beta(1)}S^{\rho}_{\nu)\beta|\rho}]_{|\alpha} + \mathcal{O}\left(\frac{h_{\rm GW}\bar{\vartheta}_{b}}{\lambda_{\rm GW}\mathcal{R}^{3}}\right),
\tag{B28}
$$

$$
{}^{(1)}C^{2}_{\mu\nu}[\bar{\vartheta}, h] = \bar{\vartheta}_{|\sigma\tau}\bar{\epsilon}_{(\mu}{}^{\sigma\alpha\beta(1)}S^{\tau}_{\nu)\beta|\alpha} + \mathcal{O}\left(\frac{h_{\rm GW}\bar{\vartheta}_{b}}{\lambda_{\rm GW}\mathcal{R}^{3}}\right),
\tag{B29}
$$

where $\bar{\vartheta}_{b}$ denotes the magnitude of the background value of the CS scalar field. The last term in Eq. (65) that we have to look at is the variation in the stress-energy tensor of the CS scalar field, $\delta T^{(\vartheta)}_{\mu\nu}[\bar{\vartheta}, \tilde{\vartheta}]$, which is given by

$$
\delta T^{(\vartheta)}_{\mu\nu}[\bar{\vartheta}, \tilde{\vartheta}] = 2\beta[\bar{\vartheta}_{|(\mu}\tilde{\vartheta}_{|\nu)} - \tfrac{1}{2}\bar{g}_{\mu\nu}\bar{\vartheta}^{|\sigma}\tilde{\vartheta}_{|\sigma}].
\tag{B30}
$$

Then, the first-order propagation equations [Eqs. (65)], assuming for simplicity that the waves travel in the absence of matter fields, can be written as

$$
\begin{aligned}
&\left\{{}^{(1)}S^{\alpha}_{\mu\nu} + \frac{\alpha}{\kappa}[\bar{\vartheta}_{|\sigma}\bar{\epsilon}_{(\mu}{}^{\sigma\alpha\beta(1)}S^{\rho}_{\nu)\beta}]_{|\rho}\right\}_{|\alpha} \\
&\quad = \frac{\beta}{\kappa}\bar{\vartheta}_{|(\mu}\tilde{\vartheta}_{|\nu)} + \mathcal{O}\left(\frac{h_{\rm GW}\bar{\vartheta}_{b}}{\lambda_{\rm GW}\mathcal{R}^{3}}, \frac{\tilde{\vartheta}_{\rm GW}}{\lambda_{\rm GW}\mathcal{R}^{3}}, \frac{\tilde{\vartheta}_{\rm GW}}{\lambda^{2}_{\rm GW}\mathcal{R}^{2}}\right).
\end{aligned}
\tag{B31}
$$

As it is clear, this propagation equation for $h_{\mu\nu}$ is coupled to the propagation equation for $\tilde{\vartheta}$ [Eq. (66)]. Notice that the right-hand side of the equations can be written as a total derivative, both in GR and in DCSMG. Also note that the second term in the right-hand side is to leading order of $\mathcal{O}(h_{\rm GW}\bar{\vartheta}_{b}/(\lambda^{3}_{\rm GW}\mathcal{R}))$.

[1] R. Jackiw and S. Y. Pi, Phys. Rev. D **68**, 104012 (2003).

[2] J. Polchinski, *Superstring Theory and Beyond*, String Theory Vol. 2 (Cambridge University Press, Cambridge, England, 1998).

[3] S. H. S. Alexander, J. Gates, and S. James, J. Cosmol. Astropart. Phys. 06 (2006) 018.

[4] V. Taveras and N. Yunes, Phys. Rev. D **78**, 064070 (2008).

[5] G. Calcagni and S. Mercuri, Phys. Rev. D **79**, 084004 (2009).
[6] S. Mercuri and V. Taveras, arXiv:0903.4407.
[7] S. Weinberg, Phys. Rev. D **77**, 123541 (2008).
[8] D. Grumiller, R. B. Mann, and R. McNees, Phys. Rev. D **78**, 081502 (2008).
[9] D. Guarrera and A. J. Hariton, Phys. Rev. D **76**, 044011 (2007).
[10] S. Alexander and N. Yunes, Phys. Rev. Lett. **99**, 241101 (2007).
[11] S. Alexander and N. Yunes, Phys. Rev. D **75**, 124022 (2007).
[12] S. Alexander, L. S. Finn, and N. Yunes, Phys. Rev. D **78**, 066005 (2008).
[13] N. Yunes and L. S. Finn, J. Phys. Conf. Ser. **154**, 012041 (2009).
[14] K. Konno, T. Matsuyama, and S. Tanda, Phys. Rev. D **76**, 024009 (2007).
[15] M. B. Cantcheff, Phys. Rev. D **78**, 025002 (2008).
[16] S. Alexander and N. Yunes, Phys. Rev. D **77**, 124040 (2008).
[17] S. H. S. Alexander, Phys. Lett. B **660**, 444 (2008).
[18] S. Alexander and J. Martin, Phys. Rev. D **71**, 063526 (2005).
[19] S. H. Alexander, M. E. Peskin, and M. M. Sheikh-Jabbari, arXiv:hep-ph/0701139.
[20] T. L. Smith, A. L. Erickcek, R. R. Caldwell, and M. Kamionkowski, Phys. Rev. D **77**, 024015 (2008).
[21] K. Konno, T. Matsuyama, Y. Asano, and S. Tanda, Phys. Rev. D **78**, 024037 (2008).
[22] N. Yunes and D. N. Spergel, Phys. Rev. D **80**, 042004 (2009).
[23] N. Yunes and C. F. Sopuerta, Phys. Rev. D **77**, 064007 (2008).
[24] D. Grumiller and N. Yunes, Phys. Rev. D **77**, 044015 (2008).
[25] N. Yunes and F. Pretorius, Phys. Rev. D **79**, 084043 (2009).
[26] M. C. Miller and E. J. M. Colbert, Int. J. Mod. Phys. D **13**, 1 (2004).
[27] M. C. Miller, Classical Quantum Gravity **26**, 094031 (2009).
[28] J. R. Gair, L. Barack, T. Creighton, C. Cutler, S. L. Larson, E. S. Phinney, and M. Vallisneri, Classical Quantum Gravity **21**, S1595 (2004).
[29] S. Vitale *et al.*, Nucl. Phys. B, Proc. Suppl. **110**, 209 (2002).
[30] K. Danzmann and A. Rudiger, Classical Quantum Gravity **20**, S1 (2003).
[31] K. Danzmann, Adv. Space Res. **32**, 1233 (2003).
[32] T. Prince, in *Proceedings of the 202nd Meeting of the American Astronomical Society* (American Astronomical Society, Washington, DC, 2003), p. 3701.
[33] LISA, http://www.esa.int/science/lisa, http://lisa.jpl.nasa.gov.
[34] D. A. Brown *et al.*, Phys. Rev. Lett. **99**, 201102 (2007).
[35] I. Mandel, D. A. Brown, J. R. Gair, and M. C. Miller, Astrophys. J. **681**, 1431 (2008).
[36] LIGO, http://www.ligo.caltech.edu.
[37] VIRGO, http://www.virgo.infn.it.
[38] Einstein Telescope, http://www.et-gw.eu.
[39] B. F. Schutz, J. Centrella, C. Cutler, and S. A. Hughes, arXiv:0903.0100.
[40] T. A. Prince *et al.*, arXiv:0903.0103.
[41] M. C. Miller *et al.*, arXiv:0903.0285.
[42] P. Amaro-Seoane *et al.*, Classical Quantum Gravity **24**, R113 (2007).
[43] T. Apostolatos, D. Kennefick, E. Poisson, and A. Ori, Phys. Rev. D **47**, 5376 (1993).
[44] C. Cutler, D. Kennefick, and E. Poisson, Phys. Rev. D **50**, 3816 (1994).
[45] D. Kennefick and A. Ori, Phys. Rev. D **53**, 4319 (1996).
[46] D. Kennefick, Phys. Rev. D **58**, 064012 (1998).
[47] Y. Mino, Phys. Rev. D **67**, 084027 (2003).
[48] S. A. Hughes, S. Drasco, E. E. Flanagan, and J. Franklin, Phys. Rev. Lett. **94**, 221101 (2005).
[49] S. Drasco and S. A. Hughes, Phys. Rev. D **73**, 024027 (2006).
[50] N. Sago, T. Tanaka, W. Hikida, and H. Nakano, Prog. Theor. Phys. **114**, 509 (2005).
[51] K. Ganz, W. Hikida, H. Nakano, N. Sago, and T. Tanaka, arXiv:gr-qc/0702054.
[52] R. Fujita, W. Hikida, and H. Tagoshi, Prog. Theor. Phys. **121**, 843 (2009).
[53] R. Ruffini and M. Sasaki, Prog. Theor. Phys. **66**, 1627 (1981).
[54] K. S. Thorne, Rev. Mod. Phys. **52**, 299 (1980).
[55] L. Barack and C. Cutler, Phys. Rev. D **69**, 082005 (2004).
[56] J. R. Gair, D. J. Kennefick, and S. L. Larson, Phys. Rev. D **72**, 084009 (2005).
[57] J. R. Gair, D. J. Kennefick, and S. L. Larson, Astrophys. J. **639**, 999 (2006).
[58] S. Babak, H. Fang, J. R. Gair, K. Glampedakis, and S. A. Hughes, Phys. Rev. D **75**, 024005 (2007).
[59] C. M. Will, Living Rev. Relativity **9**, 3 (2006), http://www.livingreviews.org/lrr-2006-3.
[60] D. Psaltis, Living Rev. Relativity **11**, 9 (2008), http://www.livingreviews.org/lrr-2008-9.
[61] N. A. Collins and S. A. Hughes, Phys. Rev. D **69**, 124022 (2004).
[62] K. Glampedakis and S. Babak, Classical Quantum Gravity **23**, 4167 (2006).
[63] C. W. Misner, K. Thorne, and J. A. Wheeler, *Gravitation* (Freeman, San Francisco, 1973).
[64] S. Alexander and N. Yunes, Phys. Rep. **480**, 1 (2009).
[65] S. Gukov, S. Kachru, X. Liu, and L. McAllister, Phys. Rev. D **69**, 086008 (2004).
[66] S. M. Carrol, *An Introduction to General Relativity, Spacetime and Geometry* (Pearson-Benjamin Cummings, San Francisco, 2003).
[67] D. M. Eardley, D. L. Lee, and A. P. Lightman, Phys. Rev. D **8**, 3308 (1973).
[68] D. M. Eardley, D. L. Lee, A. P. Lightman, R. V. Wagoner, and C. M. Will, Phys. Rev. Lett. **30**, 884 (1973).
[69] R. Wald, *General Relativity* (University of Chicago Press, Chicago, 1984).
[70] C. M. Bender and S. A. Orszag, *Asymptotic Methods and Perturbation Theory*, Advanced Mathematical Methods for Scientists and Engineers 1 (Springer, New York, 1999).
[71] N. Yunes, W. Tichy, B. J. Owen, and B. Bruegmann, Phys. Rev. D **74**, 104011 (2006).

[72] M. Bruni, L. Gualtieri, and C. F. Sopuerta, Classical Quantum Gravity **20**, 535 (2003).
[73] C. F. Sopuerta, M. Bruni, and L. Gualtieri, Phys. Rev. D **70**, 064002 (2004).
[74] A. Passamonti, M. Bruni, L. Gualtieri, and C. F. Sopuerta, Phys. Rev. D **71**, 024022 (2005).
[75] A. Passamonti, M. Bruni, L. Gualtieri, A. Nagar, and C. F. Sopuerta, Phys. Rev. D **73**, 084010 (2006).
[76] K. Konno, T. Matsuyama, and S. Tanda, arXiv:0902.4767.
[77] R. O. Hansen, J. Math. Phys. (N.Y.) **15**, 46 (1974), http://link.aip.org/link/?JMP/15/46/1.
[78] Y. Gürsel, Gen. Relativ. Gravit. **15**, 737 (1983).
[79] E. Poisson, Phys. Rev. D **54**, 5939 (1996).
[80] F. D. Ryan, Phys. Rev. D **56**, 1845 (1997).
[81] L. Barack and C. Cutler, Phys. Rev. D **75**, 042003 (2007).
[82] E. Poisson, Living Rev. Relativity **7**, 6 (2004), http://www.livingreviews.org/lrr-2004-6.
[83] S. Chandrasekhar, *The Mathematical Theory of Black Holes* (Oxford University Press, New York, 1992).
[84] W. Schmidt, Classical Quantum Gravity **19**, 2743 (2002).
[85] S. Drasco and S. A. Hughes, Phys. Rev. D **69**, 044015 (2004).
[86] N. Yunes and F. Pretorius (unpublished).
[87] A. O. Barut, *Electrodynamics and Classical Theory of Fields and Particles* (Dover, New York, 1980).
[88] J. D. Jackson, *Classical Electrodynamics* (Wiley, New York, 1999), 3rd ed.
[89] N. Yunes, C. F. Sopuerta, L. J. Rubbo, and K. Holley-Bockelmann, Astrophys. J. **675**, 604 (2008).
[90] N. Yunes and E. Berti, Phys. Rev. D **77**, 124006 (2008).
[91] W. H. Press, Phys. Rev. D **15**, 965 (1977).
[92] C. F. Sopuerta (unpublished).
[93] R. Bulirsch and J. Stoer, Numer. Math. **8**, 1 (1966).
[94] W. H. Press, B. P. Flannery, S. A. Teukolsky, and W. T. Vetterling, *Numerical Recipes: The Art of Scientific Computing* (Cambridge University Press, Cambridge, England, 1992).
[95] J. Stoer and R. Bulirsch, *Introduction to Numerical Analysis* (Springer-Verlag, New York, 1993).
[96] S. Gillessen, F. Eisenhauer, S. Trippe, T. Alexander, R. Genzel, F. Martins, and T. Ott, Astrophys. J. **692**, 1075 (2009).
[97] E. E. Flanagan and T. Hinderer, Phys. Rev. D **75**, 124007 (2007).
[98] R. A. Isaacson, Phys. Rev. **166**, 1263 (1968).
[99] R. A. Isaacson, Phys. Rev. **166**, 1272 (1968).
[100] C. M. Will and N. Yunes, Classical Quantum Gravity **21**, 4367 (2004).
[101] E. Berti, A. Buonanno, and C. M. Will, Phys. Rev. D **71**, 084025 (2005).
[102] E. Berti, A. Buonanno, and C. M. Will, Classical Quantum Gravity **22**, S943 (2005).
[103] K. G. Arun and C. M. Will, Classical Quantum Gravity **26**, 155002 (2009).
[104] L. Blanchet and T. Damour, Ann. Inst. Henri Poincare Phys. Theor. **50**, 377 (1989).
[105] T. Damour and B. R. Iyer, Ann. Inst. Henri Poincare Phys. Theor. **54**, 115 (1991).
[106] L. Blanchet, Phys. Rev. D **51**, 2559 (1995).
[107] L. Blanchet, Classical Quantum Gravity **15**, 1971 (1998).
[108] O. Poujade and L. Blanchet, Phys. Rev. D **65**, 124020 (2002).
[109] H. Stephani, D. Kramer, M. MacCallum, C. Hoenselaers, and E. Herlt, *Exact Solutions of Einstein's Field Equations* (Cambridge University Press, Cambridge, England, 2003).
[110] E. Newman and R. Penrose, J. Math. Phys. (N.Y.) **3**, 566 (1962).
[111] C. Brans and R. H. Dicke, Phys. Rev. **124**, 925 (1961).
[112] O. R. Baldwin and G. B. Jeffery, Proc. R. Soc. A **111**, 95 (1926).